JRC Scientific and Technical Reports

Validation of simplified procedures for predicting global response in the context of DBD of bridges, including the flexibility of foundations / Case study comparison of DBD iterative procedures for bridges

LESSLOSS Project / Sub-Project 8: Deliverable 112 and Deliverable 113 on Displacement-Based Design Methodologies

Fabio TAUCER, Gustavo AYALA, Carlo PAULOTTO

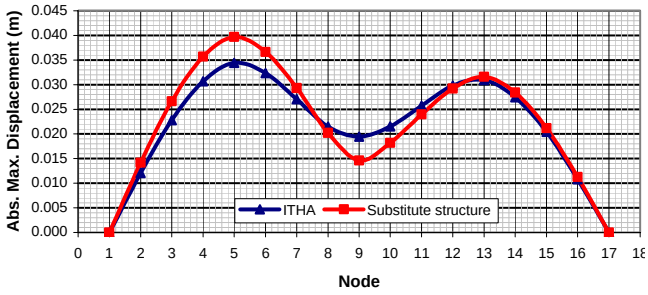

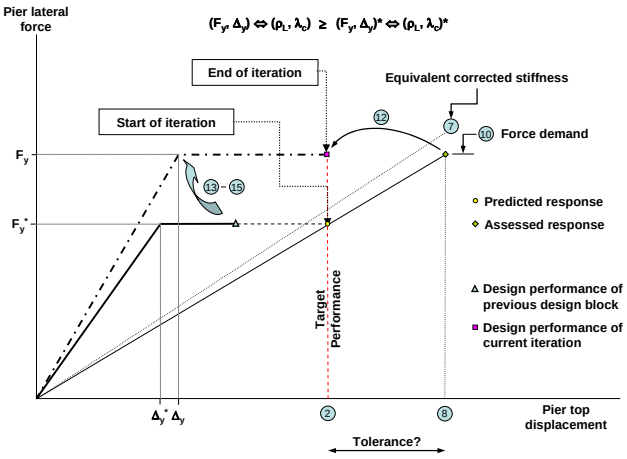

EUR 23066 EN - 2007

JRC EUROPEAN COMMISSION

ipsc Institute for the Protection and Security of the Citizen

less loss

The Institute for the Protection and Security of the Citizen provides researchbased, systems-oriented support to EU policies so as to protect the citizen against economic and technological risk. The Institute maintains and develops its expertise and networks in information, communication, space and engineering technologies in support of its mission. The strong crossfertilisation between its nuclear and non-nuclear activities strengthens the expertise it can bring to the benefit of customers in both domains.

European Commission
Joint Research Centre
Institute for the Protection and Security of the Citizen

Contact information
Address: Fabio TAUCER
E-mail: fabio.taucer@jrc.it
Tel.: +39 0332 78.5886
Fax: +39 0332 78.9049

http://ipsc.jrc.ec.europa.eu
http://www.jrc.ec.europa.eu

PUBSY 42664

EUR 23066 EN
ISSN 1018-5593

Luxembourg: Office for Official Publications of the European Communities

Printed in Italy

Validation of simplified procedures for predicting global response in the context of DBD of bridges, including the flexibility of foundations / Case study comparison of DBD iterative procedures for bridges

EXECUTIVE SUMMARY

The present report collects the work performed in Deliverable 112 "Validation of simplified procedures for predicting global response in the context of DBD of bridges, including the flexibility of foundations" and in the chapter corresponding to Displacement Based Design of Deliverable 113 "Case study comparison of DBD iterative procedures for bridges" of the LESSLOSS Project; the remaining of Deliverable 113 is published in Paulotto et al. [2007b].

The work presented herein deals with three main subjects. The first verifies that the concept of the Substitute Structure, presented in Deliverable 72 "Evaluation of Iterative DBD procedures for bridges" of LESSLOSS (Ayala et al. [2007]), constitutes a valid means of predicting the response of a bridge structure undergoing plastic deformations. The second subject is related to the formulation of a procedure for the displacement based design performance of bridges, while the third subject presents the parameters of a Takeda Model to be used within the context of non-linear time history analysis of bridges with RC rectangular hollow columns.

For the validation of the concept of the Substitute Substructure, nonlinear analysis was used as benchmark for comparing with the results of linear equivalent analysis. A series of five acceleration time histories compatible with the Eurocode 8 response spectrum were used in parametric analysis of a set of three bridge configurations with different degrees of regularity. The bridge configurations were defined from a set of real bridges designed according to Eurocode 8 as presented in Isakovic and Fishinger [2006] and related to the bridge piers tested at ELSA, as treated in Deliverable 69 "Simplified models/procedures for estimation of secant-to-yielding stiffness, equivalent damping, ultimate deformations and shear capacity of bridge piers on the basis of numerical analysis" (Paulotto et al. [2007a]).

For each bridge configuration nonlinear analysis was performed for each of the five time histories, which were scaled at three levels of peak ground acceleration, in order to induce different degrees of non-linearity, corresponding to the formation of one, two and three plastic hinges.

For the non-linear analysis a hysteretic model based on the Q-model was used, resulting in energy dissipation properties similar to those given by the linear equivalent model. For the Substitute Structure, the linear equivalent properties were derived based on the envelopes proposed in Paulotto et al. [2007a] and on a reduction factor of the target ductility, varying between 0.7 and 1.0 as a function of ductility. The combination of the modal response was done according to the procedure presented in Ayala et al. [2007].

The results show that the concept of the Substitute Structure may be used for predicting the displacement response of a regular bridge structure undergoing plastic deformations, while for irregular structures the procedure results in some discrepancies. The definition of a regular or irregular structure may be done through K-L analysis, and is work currently under development.

The confirmation of the use of the Substitute Structures gives the grounds for its use as part of the design of a structure, as presented in the section of Displacement Based Design, which proposes an iterative step-by-step procedure to design the minimum amount of steel reinforcement that meets target performance for various levels of earthquake demand or limit

states. The assessment procedure proposed in Ayala et al. [2007] and demonstrated in the present report, together with several design trials, have demonstrated the potential of the proposed design procedure; additional work is needed for further validation.

The last part of the report defines the parameters of a Takeda Model to be used in the context of non-linear time history analysis, based on the results from Paulotto et al. [2007a]. The envelope of the model is elastoplastic, while the parameters for loading and unloading are defined as a function of the longitudinal reinforcement ratio, confinement level and axial load ratio, such that the energy dissipated for different levels of ductility matches that obtained from the parametric analyses performed in Paulotto et al. [2007a]. The results from energy dissipation may also be used for defining the equivalent properties of damping within the context of the Substitute Structure.

TABLE OF CONTENTS

1. VALIDATION OF THE SUBSTITUTE STRUCTURE ASSESSMENT PROCEDURE

During the last decade there has been an increasing pressure from owners, insurance companies, politicians and engineers to re-evaluate and improve the state of practice of seismic design to meet the challenge of reducing life losses and the huge economic impact caused by recent earthquakes, which by no means could be considered as unusual or rare. As a result of this pressure, different research groups have reinitiated the investigations on the concepts and procedures for the performance-based seismic evaluation of bridges.

The idea that gave origin to the present work is based on the fact that there is a number of apparently different evaluation and design methods with which it is possible, in a simplified manner, to obtain the performance of a structure in the evaluation of existent bridges, or to guarantee the design objectives when a new one is designed, and that these methods should be further investigated and, if necessary, improved to guarantee their validity for a successful application in practice. Based on previous work developed within the group responsible of this deliverable, the premise of this investigation is that, regardless of the approximations involved in the different methods considered, the approach used for the evaluation and the design of structures may be considered as only one which, for the evaluation process considers as known the design of the structure and the seismic demand for which it needs to be evaluated, and as unknown the performance of the structure under design actions, while for the design process considers as known the target performance levels and the seismic demands and, as unknown the design parameters which guarantee such performance levels. Within this framework, it is the purpose of this work to carry out a critical review of a particular class of performance based evaluation/design methods based on displacements and to propose new alternatives which correct some of the deficiencies of existent.

The method considered in this investigation has as theoretical foundations the concepts of structural dynamics approximated to systems with non-linear behaviour, Chopra and Goel [2002], which allow, in a simple and direct way, the calculation of performances in the case of evaluation and of the correct design forces which guarantee the seismic performance objectives.

In the considered method, the original structure is substituted by a reference linear elastic structure with elements with reduced stiffness and energy dissipation characteristics consequent with the expected performance levels. This method takes into direct consideration the contribution of higher modes of vibration by using, for the calculation of performance, the complete substitute structure instead of an "equivalent" Single Degree Of Freedom (SDOF) system.

2. SELECTION OF EUROPEAN EARTHQUAKES

To carry out the inelastic step by step analyses it was necessary to have a sufficient number of earthquakes records compatible with the design demands used to design the bridges under study.

Unfortunately the number of real European records compatible with EC8 conditions is not sufficient being necessary to simulate them with an accepted procedure. After analyzing different available procedures to generate records compatible with a design spectrum it was decided to use the procedure developed by Gasparini and Vanmarcke [1976].

This procedure, to generate the artificial records compatible with a response or design spectrum considers a simulated record as a superposition of sine waves with random phase angles and amplitudes derived from a spectral density function. To simulate the transient nature of ground acceleration of real earthquakes a shape function multiplies the superposition of waves. The final simulated motion, $x(t)$, is:

$$x(t) = I(t)\sum_n A_n \operatorname{sen}(\omega_n t + \varphi_n) \tag{2.1}$$

The resulting signals are stationary in their frequency content but modulated in amplitudes. The determination of amplitudes A_n, is based on a spectral density function reflecting the relative energy contributions of the different components of the total energy of the stationary motion $x(t)$ scaled with an intensity function $I(t)$. Figure 2.1 shows the relationship between the amplitudes A_n, and their corresponding frequencies, this relationship is given by the spectral density function $G(\omega)$.

The spectral density function $G(\omega)$ may be obtained by different ways: through an auto-correlation function; through the squared Fourier amplitude spectrum; or through the procedure proposed by Gasparini and Vanmarcke [1976], based on a relationship between the spectral density function and the response spectrum of the real earthquake, i.e.:

$$G(\omega_n) = \frac{1}{\omega_n\left[\frac{\pi}{4\zeta_s} - 1\right]}\left[\frac{\omega_n^2 (S_v)_{s,p}^2}{r_{s,p}^2} - \int_0^{\omega_n} G(\omega)\,d\omega\right]^{1/2} \tag{2.2}$$

where $r_{s,p}$ is a peak factor varying between 1.25 and 3.5 for typical records and S_v is the pseudo-velocity response spectrum of a real record. To determine the spectral density function it is necessary to obtain the probability that the response of the system exceeds for the first time a given response level during a time interval Δt.

A procedure to calculate the peak factor was proposed by Vanmarcke [1976] to produce the maximum responses of a linear system exposed suddenly and for a limited time to a stationary and Gaussian excitation. This leads to the following equation:

$$r_{s,p} = \left[2\ln\left\{2n\left[1 - \exp\left(-\delta_y(\Delta t)\sqrt{\pi \ln 2n}\right)\right]\right\}\right]^{1/2} \tag{2.3}$$

where

$$n = \left[\Omega_y(\Delta t) S / 2\pi\right](-\ln p)^{-1} \tag{2.4}$$

Thus, the peak factor is a function of the spectral moments of the response $\Omega_y(\Delta t)$, $\delta_y(\Delta t)$. For small periods, these moments are the same than those for the ground motion, i.e., $\Omega_y(\Delta t) = \Omega_y \delta_y(\Delta t) = \delta$. For intermediate and large periods, the peak factor is determined from:

$$\Omega_y(\Delta t) = \omega_n \tag{2.5}$$

$$\delta_y(\Delta t) = \left(4\zeta_s / \pi\right)^{1/2} \tag{2.6}$$

where ζ_s is a time dependent fictitious damping. This damping is introduced as time dependent spectral density functions lead to better frequency contents than those which are time independent. This camping is defined as:

$$\zeta_s = \frac{\zeta}{1 - e^{-2\zeta\omega_n t}} \tag{2.7}$$

For the definition of the intensity function, $I(t)$, different shapes may be used, e.g., trapezoidal, exponential or a combination of them (Figure 2.2).

Finally, to obtain a synthetic record, the product of the sum of the sine waves by the chosen intensity function must be carried out.

3. FAMILY OF BRIDGE CONFIGURATIONS

In this report, the three-pier viaducts are analysed. These viaducts were designed according to EC8 [CEN, 2003] by Isakovic and Fishinger [2006] and are referred as V123P and V213P based on the lengths of their piers and support conditions of their superstructures. In particular viaducts V213P and V232P were analytically and experimentally investigated with results published by Pinto et al. [1996]. Figures 3.1 and 3.2 show sketches of the geometry of the evaluated bridges. The geometrical and mechanical parameters used in this evaluation are shown in Tables 3.1 and 3.2.

4. NON-LINEAR TIME HISTORY DYNAMIC ANALYSIS

To validate the results obtained from the approximate evaluation of the three bridges the non-linear step by step analyses of them were carried out using the program Drain 2DX. The maximum displacements of the piers for each of the bridges and each of the records considered as excitation were recorded and compared with the corresponding obtained with the approximate evaluation with the characteristic that the seismic demand spectra used were those directly calculated from the signals and not the smooth EC8 spectrum. The explanation of this was to deal only with the approximation of the simplified method, here used as a time history modal analysis, avoiding the interference of the errors involved in the approximation of a given mode superposition rule and the deviations of the spectra of the simulated records with respect to the target EC8 spectrum.

4.1 DESCRIPTION OF THE FEM MODEL

4.1.1 Hysteretic models

All bridge structures were analyzed using a finite element approximation in which the deck was considered as linear and formed by six beam elements of length 12.5 m. All thee piers where simulated with spring elements with non linear capabilities using as hysteresis rule that corresponding to the Q-hyst model, Saiidi and Sozen [1981].

The hysteretic model proposed by Saiidi and Sozen [1982] is defined by a hysteresis rule, based on the Takeda rule, which conveniently simulates the cyclic behaviour of reinforced concrete elements subjected to predominantly bending effects. The detailed description of the hysteresis rule is omitted in this report.

The Q model basically corresponds to a symmetric bilinear curve, in which the unloading branch has a slope equal to the elastic multiplied by $(d_y/d_{max})^a$, where d_{max} is the magnitude of the maximum inelastic excursion in any of the two directions. The reloading branches are directed to a point of the envelope with value equal to d_{max}. Figure 4.1 shows the skeleton curve for this hysteretic model.

Figure 4.2 is shown the envelop curve taken from the manual of DRAIN 2DX, where it is observed that the dashed lines that represent the unloading and reloading branches follow the rules previously mentioned.

Figure 4.3 shows the envelope curve according to the manual of Ruaumoko, where is it seen that, when there is no yielding during the previous cycle in a given direction, the reloading branch comes to the point of maximum elastic displacement at that direction, i.e. does not consider the point of maximum displacement in the opposite direction obtained during the same cycle.

Ruaumoko, in difference to DRAIN 2DX, requires as additional information the plastic hinge length. In order to match as possible the response of both programs, a plastic hinge length equal to twice the cross-section height was found to be appropriate.

In the following are shown figures where the response obtained with the two programs are compared.

In Figure 4.4 is plotted for ease of visualisation a part of the shear-displacement hysteretic behaviour of the oscillator. The blue line corresponds to the response obtained with DRAIN 2DX and the red lines to the response obtained with Ruaumoko. It can be observed that for both programs the point of first yielding of the cross-section is on the negative side of the cycle. Also, the maximum obtained displacement is approximately equal for both programs.

In the curve corresponding to the results from Ruaumoko, it is seen that as the cross-section did not yield in the previous section, the reloading branch follows a slope that points to the maximum attained displacement in that direction during the previous cycle, in this case the maximum elastic displacement in that direction.

On the contrary, in the curve corresponding to the results from DRAIN 2DX, the reloading branch follows a slope that points to the maximum inelastic displacement reached in the opposite direction during the same cycle. As this displacement is bigger than the elastic, this is the target point for the reloading branch, according to the mathematic model described above.

Because of that, DRAIN 2DX results in slightly higher displacements compared to Ruaumoko, as will be observed in the figures where the displacement are compared. Figures 4.5 and 4.6 show

respectively the displacement and shear forces obtained by both programs (only the part where inelastic behaviour occurred is shown).

4.1.2 Mass

The mass characteristics of the bridge were introduced in the model by lumping at each node the contributing mass. To simplify the application of Karhunen-Loevè analysis of the response data, the mass of the bridge was lumped at the three nodes corresponding to the heads of the piles. The comparison of the results obtained from both approaches showed negligible differences.

4.1.3 Damping properties

For linear and non-linear analyses the viscous modal damping was considered equal to 5% for all modes. In the simplified evaluation method the equivalent modal damping ratios obtained from the Shibata and Sozen [1976] approach were added to the original 5%. It is important to mention that a source of error which could not be eliminated from the non-linear step by step analysis is that due to the characteristics of method, the viscous damping characteristics of the bridges had to be introduced in the analyses through a Rayleigh damping matrix, which represents a geometric and not a physical approximation to the problem. This approach was not required for the approximate evaluation method as real modal damping ratios were directly considered.

4.2 DESCRIPTION OF THE INPUT

To carry out the analyses, the design spectrum specified by EC8 [CEN, 2003] was used, considering the viaducts are located in a soil type B. The seismic demand level considered was that corresponding to the design spectrum with 35% of the acceleration of gravity. Each bridge was subjected to three levels of earthquake, corresponding to 25%, 55% and 35% of the selected ground acceleration, as shown in Table 4.1. The first level is considered to correspond to elastic behaviour of the structure.

Figure 4.7 presents the five simulated accelerograms employed in this study. Figure 4.8 compares the response spectra of the simulated accelerograms to the EC8 response spectrum for $S = 2$, $\eta = 1$, $T_b = 0.15$ sec, $T_c = 0.50$ sec, $T_d = 2.0$ sec and $\xi = 5\%$, where slight differences between the spectra of simulated signals and the EC8 spectrum are observed. Nevertheless, the mean spectrum, also plotted in Figure 4.8, fits very well the EC8 spectrum.

5. LINEAR EQUIVALENT ANALYSIS

The simplified evaluation method has as basis the concept of the substitute structure. The substitute structure method, introduced originally by Gulkan and Sozen [1974], consists basically in the definition of a structure of equal geometric configuration as the original and linear viscoelastic properties consistent with the assumed performance under design actions. It is expected that this structure has the same performance, e.g., same maximum displacement, as the original structure, when both are subjected to the same seismic demand. It is evident that the substitute and the original structures coincide if the original does not suffer any damage when subjected to a particular seismic action. On the contrary, if the original structure suffers same damage, its corresponding substitute has different properties defined from the performance of those elements which in the original structure experience damage.

For a bridge, it is generally assumed that under the effects of the loads generated by earthquakes, the deck remains elastic and damage occurs on the piers. Under these conditions, the corresponding substitute structure may be determined using the equivalent viscoelastic properties of its damaged piers, evaluated for a particular performance. Since the dynamic response of a pier is generally dominated by its first mode unless, as for piers of significant height, the contribution of higher modes becomes important, the pier can be modelled by a SDOF oscillator, i.e., any of the methods available in the literature for SDOF oscillators may be used to determine the equivalent pier properties.

According to the authors' point of view, a substitute structure which preserves the same number of dynamic degrees of freedom as the original structure, might offer some advantages respect to those methods that reduce the original MDOF structure to a SDOF oscillator, e.g., Kowalsky [2002]. It should be noted that for some bridges the contribution of higher modes to the bridge performance can be very important and that this contribution can be hardly accounted for by using only a SDOF oscillator. Moreover, even in the cases where the SDOF substitute structure is able to approximately capture the global performance of the bridge, the tasks of defining this oscillator and rescuing the global performance of the structure from that of the single structural members may be avoided.

5.1 ANALYSIS STRATEGY

The same suite of artificial accelerograms used for the nonlinear analyses (Figure 4.7) was used also for the linear equivalent analysis described in this section. Time-history linear analysis was performed, rather than response spectrum analysis, in order to avoid the error associated to modal combination.

5.2 DESCRIPTION OF THE MODEL

The two bridge models described in chapter 3, namely V213P and V232P, were analysed. The mass, geometrical and mechanical parameters of the deck and piers of the bridge were identical to those reported in Tables 3.1 and 3.2.

5.3 EQUIVALENT PROPERTIES

The aim of this section is to describe the procedure used to calculate the equivalent viscoelastic properties of bridge piers using their basic design data affected by a correction factor to account for the transient nature of earthquake action or equations similar to those developed by Guyader and Iwan [2006]. During the validation of these equivalent properties derived from a minimization process of the error of the response results of single degree of freedom systems with equivalent properties when compared with the responses of the same systems with non-linear properties both subjected to an ensemble of simulated records compatible with the EC8 design spectrum previously discussed in this report.

This optimization process led to correction factors which lead to responses of the investigated bridges with a poor approximation when compared with those using non-linear analysis. In analyzing this deficiency it was found that the SDOF approximation could not be directly applied as a bridge pier, being a part of a bridge interacting with the deck, cannot be idealized as SDOF. To solve this problem a parametric study involving different types of bridges and a wide range of ductility demands was carried out to determining an additional correction factor to be applied to the equivalent properties derived from the SDOF assumption. Preliminary results of this investigation show the following correction factors: 0.7 for $\mu \leq 2.25$; 0.8 for $2.25 < \mu \leq 4.0$ and 0.9 for $\mu > 4.0$.

6. COMPARISON BETWEEN NONLINEAR AND LINEAR EQUIVALENT ANALYSIS

The results of the nonlinear time-history analyses and of the linear equivalent analyses are compared in terms of absolute maximum displacements in Figures 6.4 to 6.8 for Signal 1. The first two (Figures 6.4 and 6.5) correspond to bridge V123P, the following two (Figures 6.6 and 6.7) correspond to bridge V213P and the last (Figure 6.8) corresponds to bridge V232P. Following the same order, the results for Signal 2 are plotted in Figures 6.9 to 6.13, the results for Signal 3 are plotted in Figures 6.14 to 6.18, the results for Signal 4 are plotted in Figures 6.19 to 6.23 and the results for Signal 5 are plotted in Figures 6.24 to 6.28.

The dynamic properties, i.e. period and modal participation factors for the three modes of vibration of the bridge and the three stages of seismic excitation, are given in Tables 6.1 to 6.3 for Signal 1. Tables 6.1, 6.2 and 6.3 correspond respectively to bridge V123P, V213P and V232P. Following the same order, Tables 6.4 to 6.6 present the results for Signal 2, Tables 6.7 to 6.9 present the results for Signal 3, Tables 6.10 to 6.12 present the results for Signal 4 and Tables 6.13 to 6.15 present the results for Signal 5.

Note that for bridge V123P one pier yields, for bridge V213P two piers yields and for bridge V232P all piers remain elastic. Since for Bridges V213P and V232P the yield intensities of the first two piers are close, it was not possible to adjust an intensity such that would produce yielding of only one pier.

6.1 ABSOLUTE MAXIMUM DISPLACEMENTS

The results of the two types of analysis are generally in good agreement for bridge V123P and for all three stages of the considered seismic actions. The pattern of maximum displacement obtained by the two types of analysis is quite similar independently of the input accelerogram. The maximum displacements obtained with the substitute structure method are similar or slightly higher than the displacements obtained with the inelastic time-history analyses. Only for Stage 3 of Signals 4 and 5 the displacements from the time-history analyses are smaller than the displacements from the substitute structure method.

The previous observations cannot be extended to bridge V213P. Actually, in most cases the distribution of maximum displacements along the axis of the bridge is different for the two methods of analysis. Also, the values of maximum displacements obtained from the substitute structure method are in most cases smaller (up to approximately 20%) than the values resulting from the time-history analysis.

Considering the bridge V232P, the results of both methods are in quite good agreement for Signals 1, 2 and 3. For Signals 4 and 5, the substitute structure method results in displacements which are slightly smaller than the displacements obtained with the time-history analysis.

6.2 DYNAMIC PROPERTIES

Some insight on the behaviour of the examined structures might be obtained by studying their dynamic properties and the way these properties change for increasing intensity of the seismic input and for the different artificial accelerograms.

For bridge V123P the most important vibration mode, i.e. the one with the biggest modal participation factor, is the first one, followed in order of importance by the third and the second. This pattern remains constant for increasing amplitude of the input acceleration and for the five different accelerograms. Similar observations hold also for bridge V232P.

For bridge V213P and for stages 1 (0.25*0.35g – elastic behaviour) and 2 (0.55*0.35g) of the seismic intensity the most important vibration mode is the second, followed by the first and the third. This pattern changes for stage 3 (1.60*0.35g), where the first mode has the highest modal participation factor and is followed by the second and third modes. Also the relative importance of the three modes changes with increasing amplitude of the seismic action.

Based on the lengthening of the periods of the vibration modes, it is confirmed that small damage is induced on bridges V123P and V232P during the stage 2 excitation. More significant damage, evidences by increased period lengthening, is induced on the bridges for stage 3 of the earthquake amplitude. As mentioned previously, all piers of bridge V232P remain elastic, shown by the minimal change of the dynamic properties of the bridge. Among the examined artificial accelerograms, Signal 2 seems to produce the highest increase of periods in stages 2 and 3.

The results presented above serve for an initial evaluation of the proposed design method. The discussion of these results is an attempt to identify the effect of the characteristics of the bridge as well as of the seismic loading, on the accuracy of the method. Nevertheless, it would be more meaningful to extend the analysis to a statistically significant sample and to analyse the results in statistical terms, e.g. mean response and scatter, rather than on a signal-by-signal basis.

7. FLEXIBILITY OF FOUNDATIONS

The issue of the flexibility of foundations may be taken into account by modifying the stiffness and equivalent damping of the piers.

The stiffness of the pier may be modified by including at the base rotational and translational springs to account for the soil flexibility, which may be of linear or non-linear behaviour. The properties of these springs may be derived from complex models or from closed-formed solutions based on data available for the soil. The stiffness properties of the soil are combined in series with those of the pier, the properties thus obtained is used directly in the Substitute Substructure approach.

The damping given by the soil may be added up to the damping of the pier by using the Shibata and Sozen 1976 approach. This damping may be either constant, or, more realistically, non-linear, and varying as a function of the foundation deformation demands. The properties of the non-linear damping model must be obtained from complex models, for example, Finite Element Analysis, that take into account radiation damping, or from closed form expression, of which very limited information is available in present literature.

The framework for the assessment of the equivalent response of a bridge with non-linear behaviour, proposed in Ayala et al. [2007] and validated in the present report, remains valid when the flexibility of foundations is included. Therefore, the problem of including the flexibility of foundations is not so much in validating the assessment procedure, but in deriving the equivalent properties of the foundation (stiffness and damping) representative of real conditions, which are beyond the scope of the present work.

8. DISPLACEMENT-BASED DESIGN PROCEDURE

In the following, a displacement-based design procedure to meet a target performance of a bridge structure is proposed. The procedure assumes that it is possible to assess the response of a non-linear MDOF bridge structure using the concept of the substitute structure, which uses linear analysis with equivalent properties of stiffness and damping to compute peak displacement response, as described in Ayala et al. [2007] and demonstrated in Section 6 of the present report.

The target performance is defined as the maximum performance of each pier for a given level of ground shaking, and may be a maximum displacement, ductility or drift. The level of ground shaking may be associated to a peak ground acceleration, return period or magnitude of the event, and is represented by an elastic response spectrum.

The bridge structure is defined by an elastic deck with known stiffness and mass properties, and by three piers of known height L and cross section dimensions (B, H and wall thickness). The only properties that may change in the design procedure are the percentage of longitudinal steel ρ_L and the confinement level λ_c, while material properties f_y and f'_c, and the normalised axial force ν_k, remain constant.

The assessment of the response of the bridge is carried out by means of the substitute structure approach as described in Ayala et al. [2007], and is based on elastic response spectrum analysis using equivalent properties of stiffness and damping.

The equivalent stiffness and equivalent damping are evaluated from the force-displacement envelope and equivalent damping-displacement functions of the pier at the predicted response corrected by a reduction factor Λ[1].

The force-displacement envelope of the pier, which is bilinear (perfectly plastic) is defined by Δ_y and $F_y = M_y/L$, as given by the following equations:

$$\chi_y = 0.00552 \cdot \frac{\sqrt{\lambda_c}}{H} \tag{8.1}$$

$$\Delta_y = \frac{\chi_y \cdot L^2}{3} \tag{8.2}$$

$$\frac{M_y}{f'_{cm} \cdot B \cdot H^2} = 3.66 \cdot \rho_L + 0.159 \cdot \nu_k - 0.00940 \cdot \frac{H}{B} + 0.0227 \tag{8.3}$$

During the design process Δ_y and F_y vary and are functions of λ_c and ρ_L, respectively; the maximum ductility of the pier is a function of both λ_c and ρ_L.

---

[1] In the assessment procedure, the equivalent properties of the piers are computed based on predicted ductilities or displacements multiplied by a correction (reduction) factor equal or less than 1.0 and varying as a function of the ductility, type of earthquake, and other factors, such as the type of nonlinearity of members and the period of vibration of the structure. In Ayala et Al. [2007], this factor had been taken equal to 2/3, while in Section 5 of the present report this factor varies between 0.7 and 0.9, from low to large ductilities. In the iteration procedure described below it is assumed that the variation of the correction factor multiplying the predicted ductility is known and equal to Λ; the product of Λ by the predicted ductility is referred to as 'corrected ductility'. The correction factor Λ may be represented by the following equation: for $1 \leq \mu < 1.5$, $\Lambda = 1-(\mu-1)/(1+2/3)$; for $1.5 \leq \mu < 4.5$, $\Lambda = 0.7-(\mu-1.5)/15$; for $4.5 \leq \mu$, $\Lambda = 0.9$.

The equivalent damping of the pier is defined as a function of ductility and varies as a function of ρ_L. A 5% viscous damping is added to the value given from Eqs. (8.4) and (8.5); the same amount of damping is assigned to the deck.

$$\eta = \left[1 - \frac{\nu_k - 0.1}{78 \cdot \rho_L}\right] \cdot 0.96 \cdot \rho_L^{0.2} \cdot \left[1 - \frac{1}{\sqrt{\mu}}\right] \tag{8.4}$$

$$\xi_{eq} = 3\eta \frac{\mu}{\mu_\Delta} \cdot \frac{L_p}{L} \tag{8.5}$$

$$\mu_\Delta = 1 + (\mu - 1)\left[\frac{3L_p}{L}\left(1 - 0.5\frac{L_p}{L}\right)\right] \tag{8.6}$$

$$\begin{cases} \dfrac{L_p}{L} = c_L \cdot \dfrac{\mu - 1}{\mu_L - 1} & \text{with} \quad 1 \le \mu \le \mu_L \\ \dfrac{L_p}{L} = c_L & \text{with} \quad \mu \ge \mu_L \end{cases} \tag{8.6}$$

where c_L and μ_L are two parameters that depend on the shear span-to-depth ratio a/d, and are equal, for the medium and tall piers (a/d equal to 3.5 and 5.3), to 0.0624 and 9, and for the short pier (a/d equal to 1.8), to 0.127 and 5, respectively. Equation (8.6) considers that the post-yielding to initial stiffness of the section is equal to zero.

The design procedure is iterative and varies ρ_L and λ_c so that the maximum response of each pier does not exceed the target performance at different levels of ground shaking using minimum percentages of steel reinforcement while providing sufficient capacity against the demands from gravity and service loads.

Note that the value of the energy dissipated at the section level may be alternatively calculated with more accuracy by using the expression available for computing the energy dissipated by the Takeda Model, assuming $\beta = 0.3$ and α from Figure 9.6 or from Eq. (9.2)

Step-by-step design procedure

The first phase of the design procedure is to define the initial envelopes of each pier (*i.e.*, ρ_L and λ_c) so that gravity and serviceability earthquake loads can be resisted by the piers without entering into the nonlinear range, thus defining the minimum values of F_y and Δ_y of each pier during the design procedure. In this phase Δ_y may be computed assuming λ_c equal to 1.0, while the calculation of the demands on the bridge may be carried out assuming an effective damping of 5% and a response spectrum for the serviceability earthquake with a reduction factor of the seismic forces (q factor) equal to 1.0.

The second phase is constituted by a series of iterative design blocks, each block corresponding to a particular ground shaking level and target performance for which a design is sought. Within each design block, the design values obtained from the previous design block (*i.e.*, for a lower level of ground shaking, or, for the first block, for serviceability and gravity loads), ρ_L^* and λ_c^* cannot be decreased, thus setting the minimum strength, deformation and energy dissipation capacity to be maintained during the iteration procedure at a given design block.

The ground shaking is represented by a smooth or multi-linear elastic response spectrum defined at different levels of equivalent damping.

The step-by-step iteration procedure in each design block is as follows:

Step 1. Start the procedure by assuming an initial distribution of displacements at the top of the piers, equal to the target performance of the bridge.

Step 2. Update the displacement shape. For the first iteration the displacement shape is equal to that assumed in Step 1, while for subsequent iterations the displacement shape is equal to the design displacements obtained from Step 12 in the previous iteration.

Step 3. Update the force-displacement envelopes (bi-linear diagrams, Δ_y and F_y) and equivalent damping-displacement functions of each pier corresponding to ρ_L and λ_e. For the first iteration, these are equal to those obtained from the previous design block (Δ_y^* and F_y^*, and equivalent damping corresponding to ρ_L^* and λ_e^*); for the first design block the gravity and serviceability load design is used. For iterations other than the first, the force-displacement envelopes and equivalent damping-displacement functions are equal to those computed in Step 15 of the previous iteration.

Step 4. Evaluate for the displacement shape of Step 2, the secant stiffness of each pier using the force-displacement envelopes from Step 3.

Step 5. Evaluate the ductility demands at each pier from the displacement shape of Step 2 and the yield displacements Δ_y from Step 3.

Step 6. Compute the correction factor Λ to be applied to each pier as a function of the ductility evaluated in Step 5.

Step 7. Evaluate the corrected equivalent stiffness and corrected equivalent damping of each pier based on the force-displacement envelopes and damping-displacement functions from Step 3 computed from the displaced shape of Step 2 modified by the correction factor from Step 6.

Step 8. Evaluate the response of the structure by means of response spectrum modal linear analysis using the corrected equivalent properties of Step 7, and obtain the displacement shape of the structure. The modal damping is computed as the sum of the corrected equivalent damping of each pier weighted by its energy contribution within each mode, including the damping contribution of the deck.

Step 9. Check if the displaced shape obtained from Step 8 is within tolerance with respect to the displaced shape assumed in Step 2. If the check between predicted and assessed displacements is within tolerance, then the procedure has converged, else, go to the next step.

Step 10. Evaluate the force demand on each pier corresponding to the displacement shape obtained in Step 8 using the secant stiffness from Step 4, and compute the percentage difference of this force with respect to F_y^*.

Step 11. Compute the percentage difference between the displacements obtained in Step 8 and the target performance.

Step 12. Compute the design forces and design displacements of each pier. For each pier, if the displacement obtained in Step 8 is larger than the target performance, the design

displacement is made equal to the target performance and the design force is made equal to the force demand computed in Step 10, else, the force demand obtained in Step 10 is compared with F_y^*. If the force demand from Step 10 is larger than F_y^*, then the percentage differences in force and displacement computed in Step 10 and Step 11 are compared to compute the design forces and displacements. If the percentage difference in displacement is smaller than the percentage difference in force, then the design displacement is made equal to the target performance and the design force is made equal to the force demand computed in Step 10, else, the design displacement is made equal to the displacement obtained in Step 8 and the design force is made equal to the force corresponding to this displacement based on the force-displacement envelope corresponding to Δ_y^* and F_y^*. If the force demand from Step 10 is smaller than F_y^*, then the same design strategy applied when the percentage difference in force is smaller than that in displacement is applied.

Step 13. Compute the percentage of longitudinal steel ρ_L of the piers required to meet the design forces computed in Step 12. If the design force falls on the force-displacement envelope corresponding to Δ_y^* and F_y^*, ρ_L is equal to ρ_L^*.

Step 14. Compute the confinement level λ_c required for each pier to reach the design displacements of Step 12 considering the percentage of longitudinal steel ρ_L computed in Step 13 using the charts of Figure 8.1 (in terms of ductility) or Figure 8.2 (in terms of drifts). The ductility and drift used in the charts is derived from the design displacement of Step 12 (for computing the ductility, on or two iterations may be needed in entering the chart of Figure 8.1, as Δ_y is a function of λ_c). If the design displacement is less than the design displacement performance obtained from the pervious design block, λ_c is equal to λ_c^*.

Step 15. Compute the force-displacement envelopes and equivalent damping-displacement functions for each pier based on the ρ_L and λ_c values obtained in Step 13 and Step 14.

Step 16. Go to Step 2.

The result from the design iteration procedure is a set of ρ_L and λ_c values for each pier so that the target performance is met at each level of ground shaking with the minimum possible amounts of steel reinforcement.

It is important to mention that the whole design procedure can be simplified by assuming that Δ_y remains independent of λ_c. This may be done by computing Δ_y for an average λ_c value of 1.5, and updating Δ_y only at the end of the iteration procedure.

A graphical representation of the iteration procedure is shown in Figure 8.3, starting with the first iteration from a previous converged design block, and considering that the assessed displacement obtained in Step 8 is larger than the target performance.

In Figure 8.4, the different design possibilities described in Step 12 that may take place depending on the response of the structure with respect to the target performance and the design force form the previous design block are presented.

The assessment procedure proposed in Ayala et al. [2007] and demonstrated in Section 6, together with several design trials, have demonstrated the potential of the proposed design procedure; additional work is proposed for further validation.

The reliability of the design method depends on two conditions: the ability of the design method in converging to an optimum design solution, and the ability of the assessment procedure in predicting the non-linear response of the bridge. Accepting that the design method will converge to an optimum solution, the reliability related to the second condition may be taken into account by modifying the target performance. For irregular bridges, where the assessment procedure based on the substitute structure may give displacement demands lower than those obtained from a non-linear time history analysis, the bridge may be designed to a target performance reduced by an amount equal to this difference (resulting in higher secant-to-yield stiffness and yield strength), while ensuring a deformation capacity of the section compatible with the unreduced target performance (resulting in higher confinement).

9. PARAMETERS OF THE TAKEDA MODEL FOR NON-LINEAR TIME HISTORY ANALYSIS

This section defines the parameters of a Takeda model to be used in the context of non-linear time history analysis to assess the earthquake response of a bridge structure with rectangular RC hollow piers, assuming that the following properties are known: H, B, L, ν_k, ρ_L and λ_c.

The Takeda Model is defined by a moment-rotation envelope and by two factors, α and β, that determine the rules for cyclic loading and unloading.

The moment-rotation envelope is defined by $\theta_y=\chi_y L_p$ and M_y, as given by Eqs. (8.1), (8.3) and (8.4). The ratio of the post-yielding to initial stiffness r is set equal to zero, reflecting the results obtained from the parametric analysis performed in Paulotto et al. [2007a].

The parameters α and β are chosen such that the energy ξ_{eq} dissipated by the Takeda model, as given by the expression proposed by Loading et al. [1998] in Eq. (9.1), is equal to the energy dissipated η by the section as obtained from cyclic numerical analysis performed on a fibre model at different levels of ductility as described in Paulotto et al. [2007a].

$$\xi_{eq} = \xi_0 + \frac{2}{\pi}\left\{1-\frac{3}{4}\mu^{\alpha-1}-\frac{1}{4}\left[\frac{r\beta\mu}{\gamma}\left(1-\frac{1}{\mu}\right)+1\right]\left[2-\beta\cdot\left(1-\frac{1}{\mu}\right)\right] -\mu^{\alpha-1}\gamma-\frac{1}{4}\left[\frac{r\beta^2\mu}{\gamma}\left(1-\frac{1}{\mu}\right)^2\right]\right\} \tag{9.1}$$

where $\gamma = r\mu - r + 1$, α is the unloading stiffness factor and β is the reloading stiffness factor. The values of α and β are calculated for ξ_0 equal to zero, i.e., only the contribution of hysteretic damping is taken into account.

The energy dissipated by the numerical analyses is best fitted by Eq. (9.1) by setting β constant and equal to 0.3 and varying α between 0.01 and 0.93 as a function of the amount of longitudinal reinforcement ρ_L and the axial load ratio ν_k, as given in Table 9.1. and represented in graphical form in Figure 9.6. The comparison between the energy dissipated by the Takeda model using the α values given in Table 9.1 and the energy η dissipated by the Fibre model is shown in Figure 9.1 through Figure 9.5, for ρ_L varying between 0.005 and 0.04 and ν_k varying between 0.1 and 0.4, for section ductility values varying up to 12.

The values of α given in Table 9.1 may be fitted by a closed form expression as a function of ν_k and ρ_L:

$$\alpha = 1.1\nu_k - 7.2\left(\rho_L - 0.005\right)^{0.73} + 0.53 \qquad (9.2)$$

The comparison between the α values given by Eq. (9.2) and those given by Table 9.1 is represented in Figure 9.12, while the comparison between the energy dissipated by the Takeda model using the α values given in Eq. (9.2) and the energy η dissipated by the Fibre model is shown in Figure 9.7 through Figure 9.11, showing that the error in the approximation of Eq. (9.2) is acceptable, with the exception of the case where ρ_L: is equal to 0.005, where a larger error is obtained for high values of ν_k.

10. CONCLUSION

This report presented the results of a simplified seismic performance evaluation method using equivalent viscoelastic parameters. This method is based on the concept of the substitute structure from which the maximum displacements of the piers of a bridge under a given seismic loading can be determined.

Throughout this report it is shown that the linearization of an originally non-linear problem by means of equivalent viscoelastic properties for the piers of a bridge, where all non-linear effects due to seismic action are assumed to occur, may be a practical and sufficiently approximated tool for the seismic evaluation, and ultimately for the displacement-based design.

It is shown that by using this improved substitute structure method with equivalent linear parameters, derived with a logical procedure that accounts for the randomness of the response, it is possible to obtain results with better approximation that those obtained with the conventional substitute structure methods.

The work presented herein shows that the structural evaluation according to the proposed methods gives acceptable results with a limited computational effort, as long as the structure is regular. Unfortunately, this conclusion can not be extended to the case of irregular bridges, where it is shown, particularly in the second example, that the modes which are important for the structural response change with the seismic intensity.

The proposed method can be considered as an improved version of other methods currently in use, or under investigation by other research groups, as it takes into consideration the contribution of higher modes of vibration and the displacement reversal nature of earthquake action through evolving modal spectral analyses, rather than from evolving force or displacement based pushover analyses.

It is demonstrated that the use of smooth response spectrum as seismic demand does not guarantee sufficient accuracy, or even correct results, for all situations. For instance, the results presented in this document for the V213P bridge are not satisfactory when compared with those of the statistical study of many non-linear time history analyses. The observed lack of approximation may be due to the fact that, for the considered design level, the bridge, due to the occurrence of new damage, changed its fundamental mode shape from a rotational to a translational type. It is evident that more research efforts are needed to fully understand why this

lack of approximation occurs, to determine for which combinations of bridge configurations and seismic design levels the application of the proposed methods is reliable.

It is shown that the application of this method is simpler than that of other methods, as all calculations involved may be carried out with commercial analysis software. Furthermore, the application of modal spectral analysis with accepted mode combination rules for the evaluation of bridges gives evaluations and designs corresponding to maximum expected performances.

The report also presents a displacement-based procedure for the design of a bridge structure, using as basis the concept of the substitute structure for assessing the response of trial designs. The method is iterative and aims at obtaining the optimum design of the piers (longitudinal reinforcement and confinement ratio) to meet the target performance of the bridge (pier or section ductility, or pier displacement or drift) defined at different levels of earthquake demand (peak ground accelerations related to different limit states).

Lastly, the report defines the parameters of a Takeda Model to be used in the context of non-linear time history analysis to assess the earthquake response of a bridge structure with rectangular RC hollow piers. The definition of the parameters is also useful in the context of the substitute structure, as it proposes a closed form solution for defining the energy dissipated by the piers as a function of ductility considering the design of the piers (longitudinal reinforcement ratio) and the axial load ratio.

11. RECOMMENDATIONS

Some of the deficiencies of currently applied equivalent viscoelastic parameters in seismic performance evaluation methods which need to be further investigated are:

- There is no sufficient theoretical and/or numerical basis for most of currently used equations for equivalent damping.
- The use of initial or secant stiffness as an estimator of effective stiffness may lead to erroneous results related to the regularity condition of the bridge.
- Equivalent viscoelastic properties are interrelated, thus the modification of one of them requires most of the times the modification of the other.
- The equivalent secant stiffness and damping are being derived for full cyclic conditions and under the assumption that the non-linear structural element, part of a structure, may be idealized by a linear SDOF system.
- Damping is smeared throughout all structural elements as modal damping using a procedure which allows energy dissipation throughout the structure and not only by the elements which present damage
- Stiffness and strength degradation are not normally considered.

In the present work, and in various published works, it is shown that under certain circumstances, all employed methods fail to produce acceptable results. It is shown that for the

considered structures, there exists a condition of regularity which is related not only to the geometric characteristics, but also to the general characteristics of the seismic demand, beyond which the obtained evaluation results become incorrect. The investigation involved in the formulation of the proposed method has tried with limited success to eliminate this drawback; nevertheless this problem is currently under investigation.

In future research, it would be meaningful to extend the study to a statistically significant sample and to analyse the results in statistical terms, e.g. mean response and scatter, rather than on a signal-by-signal basis.

Concerning the displacement based design procedure, it is recommended to perform a parametric study on the ability of the procedure for converging towards a solution for different types of bridge configurations and limit states, and on its efficiency considering the number of iterations required to reach a solution.

REFERENCES

Ayala G., Paulotto C. and Taucer F. [2007] "Evaluation of Iterative DBD procedures for bridges", *JRC Scientific and Technical Reports*, EUR 22888 EN, European Commission, Ispra, Italy.

CEN [2003] "Eurocode 8. Design of structures for earthquake resistance - Part 1: General Rules, seismic actions and rules for buildings*", prEN 1998-1*, Commission of the European Communities, Brussels, Belgium.

Chopra A. K. and Goel R. K. [2002] "A modal pushover analysis procedure for estimating seismic demands for buildings", *Earthquake Engineering and Structural Dynamics*, Vol. 31, pp. 561-582.

Gasparini D. A. and Vanmarcke E. H. [1976] "Simulated earthquake motions compatible with prescribed response spectra", Civil Engineering Research Report R76-4, *Massachusetts Institute of Technology*, Cambridge, USA.

Gulkan P. and Sozen M. A. [1974] "Inelastic Responses of Reinforced Concrete Structures to Earthquakes Motions", *Proceedings of the ACI*, Vol. 71, No. 12, pp. 604-610.

Guyader C. and Iwan W. D. [2006] "Determining equivalent linear parameters for use in a capacity spectrum method of analysis", *Journal of Structural Engineering*, ASCE, Vol. 132, No. 1, pp. 59-67.

Isakovic T. and Fishinger M. [2006] "*Higher modes in simplified inelastic seismic analysis of single column bent viaducts*", Earthquake Engineering and Structural Dynamics, Vol. 35, pp. 95-114.

Kowalsky M. J. [2002] "A displacement-based approach for the seismic design of continuous concrete bridges", *Earthquake Engineering and Structural Dynamics*, Vol. 31, pp.719-747.

Paulotto C., Ayala G. and Taucer F. [2007a] "Simplified models/procedures for estimation of secant-to-yielding stiffness, equivalent damping, ultimate deformations and shear capacity of bridge piers on the basis of numerical analysis", *JRC Scientific and Technical Reports*, EUR 22894 EN, European Commission, Ispra, Italy.

Paulotto C., Ayala G. and Taucer F. [2007b] "Displacement based design methodologies for bridges", *JRC Scientific and Technical Reports*, EUR 22885 EN, European Commission, Ispra, Italy.

Pinto A. V., Verzeletti G., Pegon P. Magonette G., Negro P., Guedes J. [1996] "Pseudo-Dynamic Testing of Lange Scale R/C Bridges", *JRC Scientific and Technical Reports*, EUR 16378 EN, European Commission, Ispra, Italy.

Saiidi M. and Sozen M. A. [1981] "Simple nonlinear seismic analysis of R/C structures", *Journal of Structural Division*, ASCE, Vol. 107, pp 937-952.

Shibata A. and Sozen M. A. [1976] "Substitute-structure method for seismic design in R/C", *Journal of the Structural Division*, ASCE, Vol. 102, No. ST1.

Vanmarcke E. H. [1976], *Seismic risk and engineering decisions*, Ed. Elsevier Publishing Co, New York.

TABLES

Table 3.1 Geometrical and mechanical properties of superstructure

Viaduct	M (ton)	M_1 (ton)	M_2(ton)	M_3 (ton)	Cross area (m^2)	Inertia (m^4)
V123P	254.8	329.0	291.9	366.0	6.48	87.24
V213P	254.8	329.0	291.9	366.0	6.48	87.24

Table 3.2 Geometrical and mechanical properties piers

Viaduct	Column	h (m)	A (m^2)	Δ_y (m)	I_{cr} (m^4)	I_u (m^4)
V123P	c1	7.0	4.16	0.01491	3.63	1.307
	c2	14.0	4.16	0.03766	2.17	0.173
	c3	21.0	4.16	0.06657	2.26	0.113
V213P	c1	14.0	4.16	0.02898	2.22	0.111
	c2	7.0	4.16	0.01127	2.40	0.192
	c3	21.0	4.16	0.06657	2.26	0.113

Table 4.1 Normalized performance intensities using in the simplified analyses of the bridges

Stage	Acceleration
Stage 1 (elastic)	0.25*(0.35g)
Stage 2	0.55*(0.35g)
Stage 3	1.60*(0.35g)

Table 6.1 Dynamic properties of bridge V123P, signal 1

	Mode	Period (s)	Modal participation factor
Stage 1	First	0.7259	-48.168
	Second	0.3223	-13.501
	Third	0.1857	27.887
Stage 2	First	0.7387	-48.25
	Second	0.3236	-13.09
	Third	0.1858	27.93
Stage 3	First	0.8911	-49.15
	Second	0.3427	-12.21
	Third	0.2044	26.74

Table 6.2 Dynamic properties of bridge V213P, signal 1

	Mode	Period (s)	Modal participation factor
Stage 1	First	0.5259	23.20
	Second	0.4358	50.26
	Third	0.2048	-14.68
Stage 2	First	0.5455	36.19
	Second	0.4920	43.77
	Third	0.2322	-7.37
Stage 3	First	0.7363	-56.92
	Second	0.5429	4.97
	Third	0.2658	3.82

Table 6.3 Dynamic properties of bridge V232P, signal 1

	Mode	Period (s)	Modal participation factor
Stage 1	First	0.8193	-55.84
	Second	0.4412	0.00
	Third	0.2740	14.09
Stage 3	First	0.8193	-55.84
	Second	0.4412	0.00
	Third	0.2740	14.09

Table 6.4 Dynamic properties of bridge V123P, signal 2

	Mode	Period (s)	Modal participation factor
Stage 1	First	0.7295	-48.168
	Second	0.3223	-13.501
	Third	0.1857	27.887
Stage 2	First	0.7444	-48.30
	Second	0.3244	-12.85
	Third	0.1858	27.95
Stage 3	First	0.9100	-49.26
	Second	0.3449	-12.11
	Third	0.2068	26.57

Table 6.5 Dynamic properties of bridge V213P, signal 2

	Mode	Period (s)	Modal participation factor
Stage 1	First	0.5259	23.20
	Second	0.4358	50.26
	Third	0.2048	-14.68
Stage 2	First	0.5444	36.66
	Second	0.4818	43.36
	Third	0.2313	-7.43
Stage 3	First	0.6209	54.62
	Second	0.5242	17.20
	Third	0.2535	-0.307

Table 6.6 Dynamic properties of bridge V232P, signal 2

	Mode	Period (s)	Modal participation factor
Stage 1	First	0.8193	-55.84
	Second	0.4412	0.00
	Third	0.2740	14.09
Stage 3	First	0.9597	-56.17
	Second	0.4770	0.00
	Third	0.2792	12.70

Table 6.7 Dynamic properties of bridge V123P, signal 3

	Mode	Period (s)	Modal participation factor
Stage 1	First	0.7295	-48.168
	Second	0.3223	-13.501
	Third	0.1857	27.887
Stage 2	First	0.7404	-48.27
	Second	0.3239	-13.02
	Third	0.1858	27.94
Stage 3	First	0.8982	-49.59
	Second	0.3499	-13.44
	Third	0.2181	25.29

Table 6.8 Dynamic properties of bridge V213P, signal 3

	Mode	Period (s)	Modal participation factor
Stage 1	First	0.5259	23.20
	Second	0.4358	50.26
	Third	0.2048	-14.68
Stage 2	First	0.5407	34.00
	Second	0.4752	45.31
	Third	0.2282	-8.39
Stage 3	First	0.7469	-56.10
	Second	0.5269	10.49
	Third	0.2666	4.780

Table 6.9 Dynamic properties of bridge V232P, signal 3

	Mode	Period (s)	Modal participation factor
Stage 1	First	0.8193	-55.84
	Second	0.4412	0.00
	Third	0.2740	14.09
Stage 3	First	0.9736	-56.20
	Second	0.4801	0.00
	Third	0.2796	12.59

Table 6.10 Dynamic properties of bridge V123P, signal 4

	Mode	Period (s)	Modal participation factor
Stage 1	First	0.7295	-48.168
	Second	0.3223	-13.501
	Third	0.1857	27.887
Stage 2	First	0.7544	-48.38
	Second	0.3257	-12.44
	Third	0.1858	28.00
Stage 3	First	0.9129	-49.05
	Second	0.3421	-11.54
	Third	0.1997	27.21

Table 6.11 Dynamic properties of bridge V213P, signal 4

	Mode	Period (s)	Modal participation factor
Stage 1	First	0.5259	23.20
	Second	0.4358	50.26
	Third	0.2048	-14.68
Stage 2	First	0.5364	30.89
	Second	0.4659	47.23
	Third	0.2236	-9.72
Stage 3	First	0.7584	-56.35
	Second	0.5313	8.97
	Third	0.2674	4.94

Table 6.12 Dynamic properties of bridge V232P, signal 4

	Mode	Period (s)	Modal participation factor
Stage 1	First	0.8193	-55.84
	Second	0.4412	0.00
	Third	0.2740	14.09
Stage 3	First	0.9982	-56.23
	Second	0.4849	0.00
	Third	0.2802	12.45

Table 6.13 Dynamic properties of bridge V123P, signal 5

	Mode	Period (s)	Modal participation factor
Stage 1	First	0.7295	-48.168
	Second	0.3223	-13.501
	Third	0.1857	27.887
Stage 2	First	0.7392	-48.25
	Second	0.3237	-13.07
	Third	0.1858	27.93
Stage 3	First	0.8278	-48.71
	Second	0.3340	-12.04
	Third	0.1928	27.61

Table 6.14 Dynamic properties of bridge V213P, signal 5

	Mode	Period (s)	Modal participation factor
Stage 1	First	0.5259	23.20
	Second	0.4358	50.26
	Third	0.2048	-14.68
Stage 2	First	0.5367	32.10
	Second	0.4637	46.48
	Third	0.2243	-9.43
Stage 3	First	0.6121	53.50
	Second	0.5226	20.41
	Third	0.2515	-1.073

Table 6.15 Dynamic properties of bridge V232P, signal 5

	Mode	Period (s)	Modal participation factor
Stage 1	First	0.8193	-55.84
	Second	0.4412	0.00
	Third	0.2740	14.09
Stage 3	First	1.0867	-56.34
	Second	0.5015	0.00
	Third	0.2822	11.92

Table 9.1 α values as a function of longitudinal reinforcement ρ_L and axial load ratio ν_k

ν_k	ρ_L				
	0.005	**0.01**	**0.02**	**0.03**	**0.04**
0.1	0.62	0.47	0.28	0.13	0.01
0.2	0.79	0.61	0.41	0.26	0.13
0.3	0.88	0.75	0.54	0.39	0.27
0.4	0.93	0.82	0.64	0.47	0.33

FIGURES

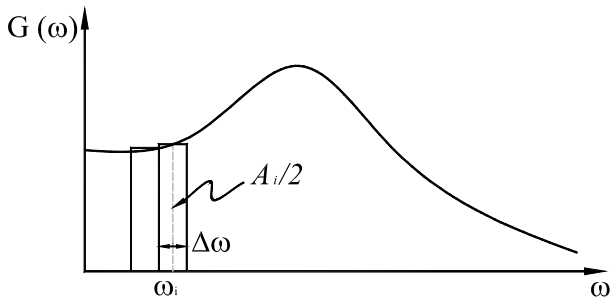

Figure 2.1. Spectral density function

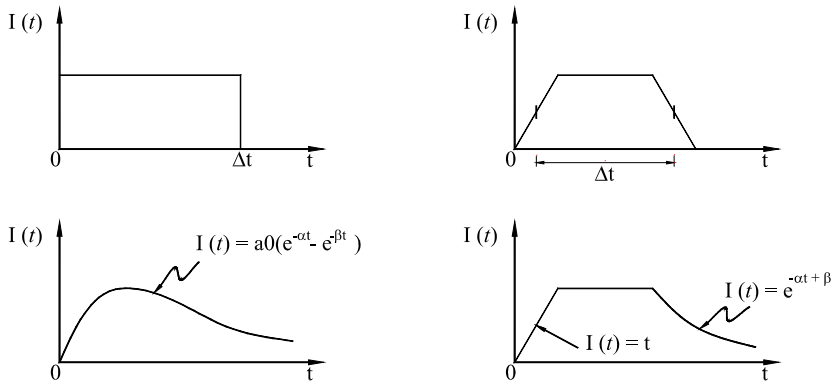

Figure 2.2. Commonly used intensity functions

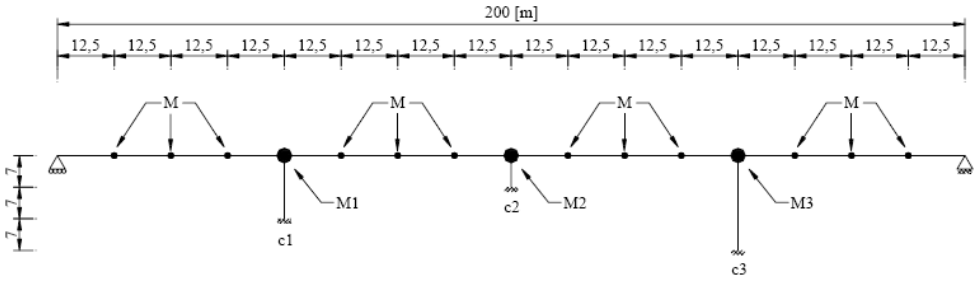

Figure 3.1. Geometry and location masses of the of bridge V213P

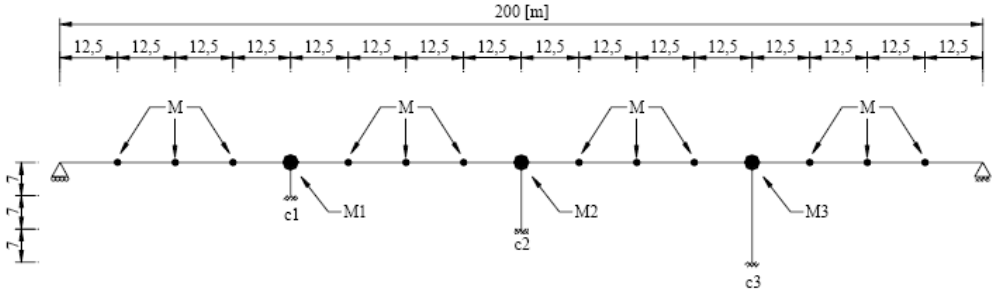

Figure 3.2. Geometry and location masses of the of bridge V123P

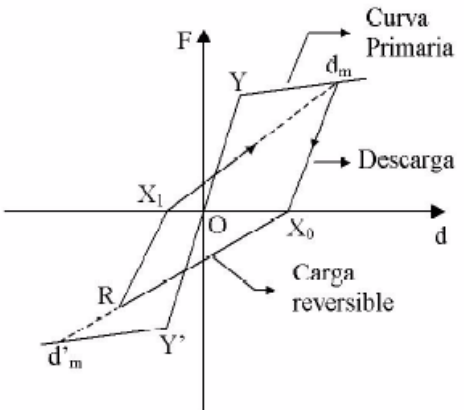

Figure 4.1. Q-Hysteretic model proposed by Saiidi and Sozen [1981]

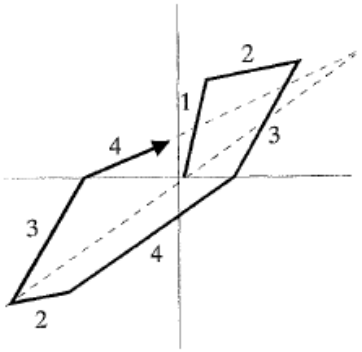

Figure 4.2. Q-Hysteretic model, DRAIN 2DX

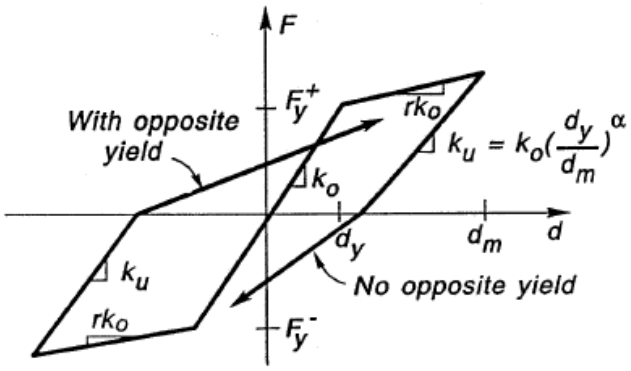

Figure 4.3. Q-Hysteretic model, Ruaumoko

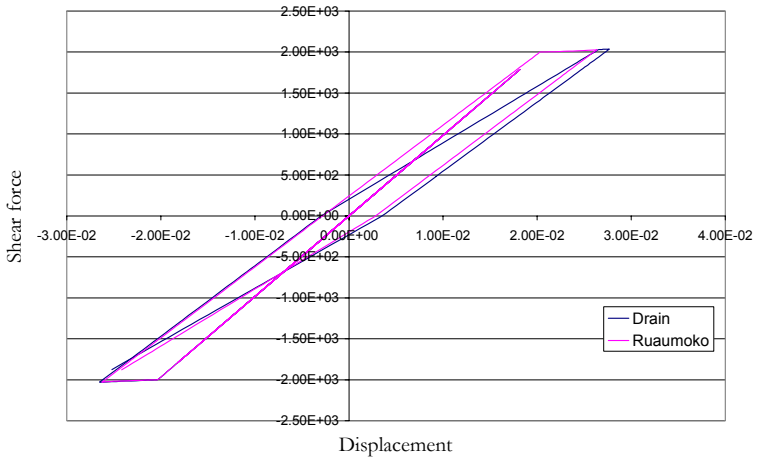

Figure 4.4. Force-displacement curves from Drain 2DX and Ruaumoko

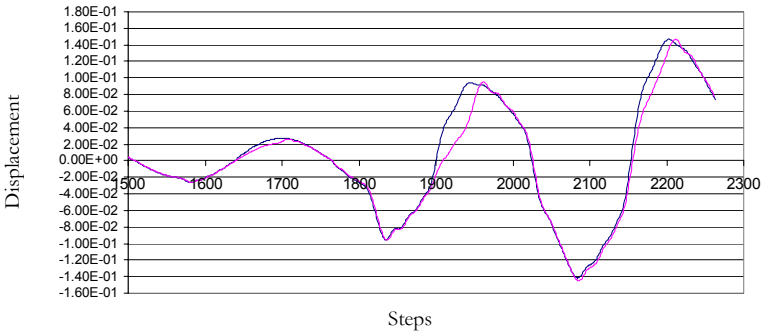

Figure 4.5. Drain (blue) and Ruaumoko (red)

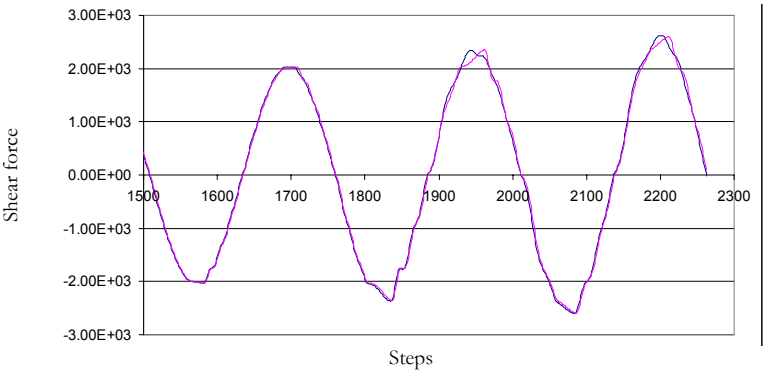

Figure 4.6. Shear force from Drain 2DX (blue line) and Ruaumoko (red line)

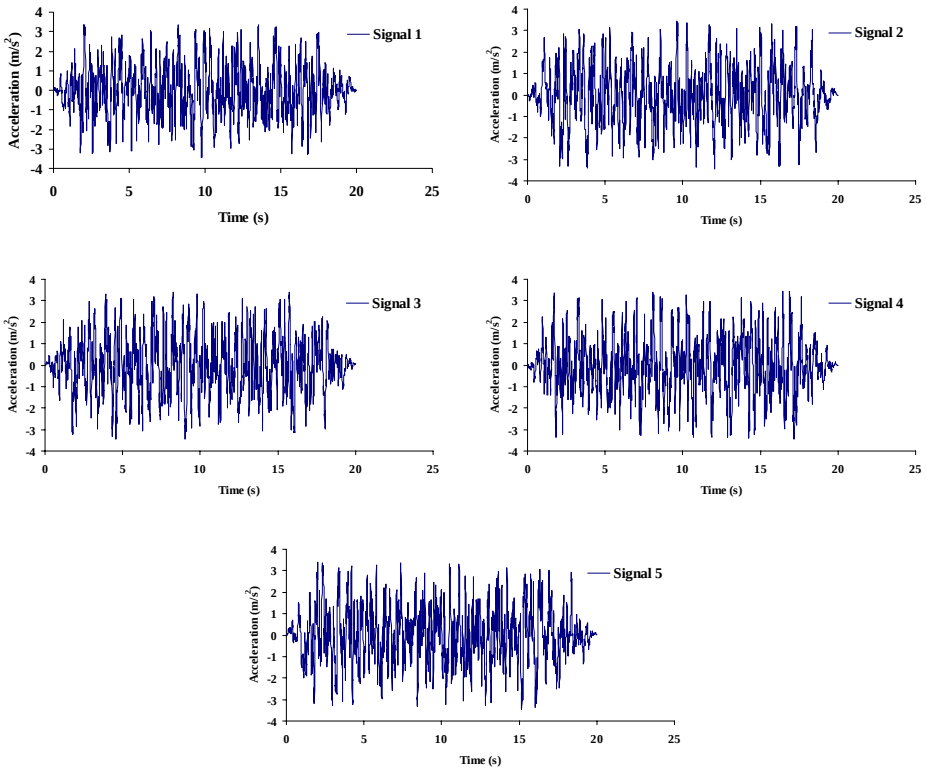

Figure 4.7.Used simulated records

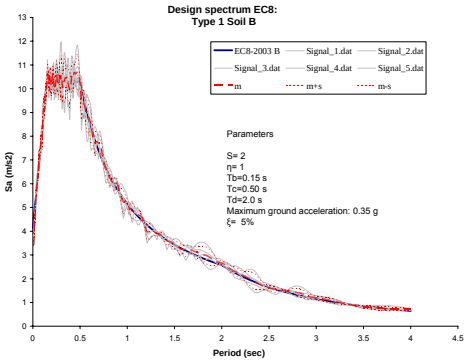

Figure 4.8. Comparison of the EC8 elastic response spectrum with the elastic response spectra for the five considered signals and their mean value

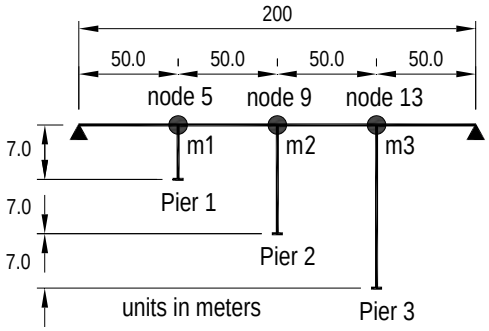

Figure 6.1. Geometry of bridge V123P

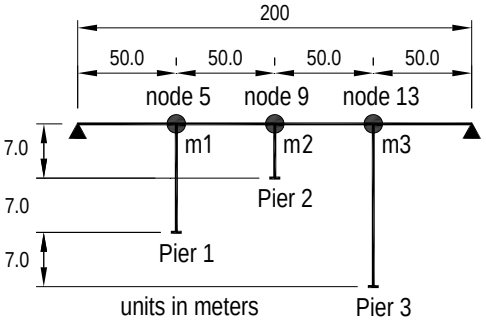

Figure 6.2. Geometry of bridge V213P

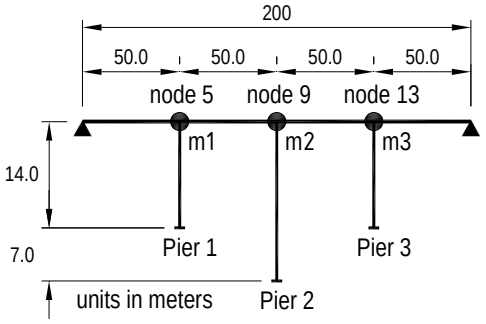

Figure 6.3. Geometry of bridge V232P

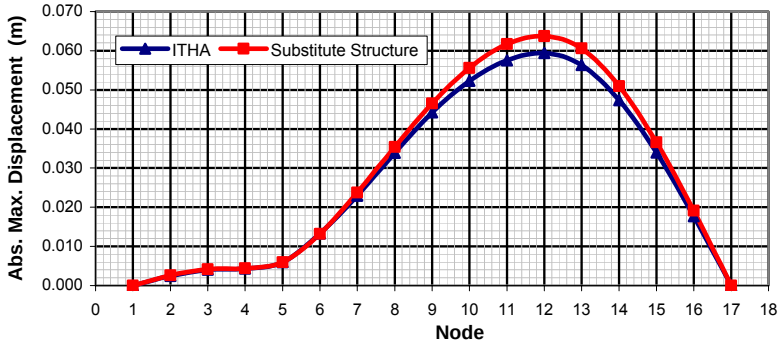

Figure 6.4. Distribution of absolute maximum displacements of bridge V123P, stage 2, signal 1

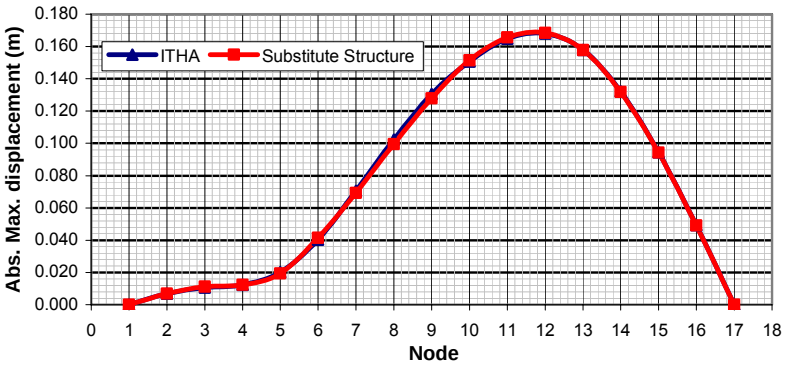

Figure 6.5. Distribution of absolute maximum displacements of bridge V123P, stage 3, signal 1

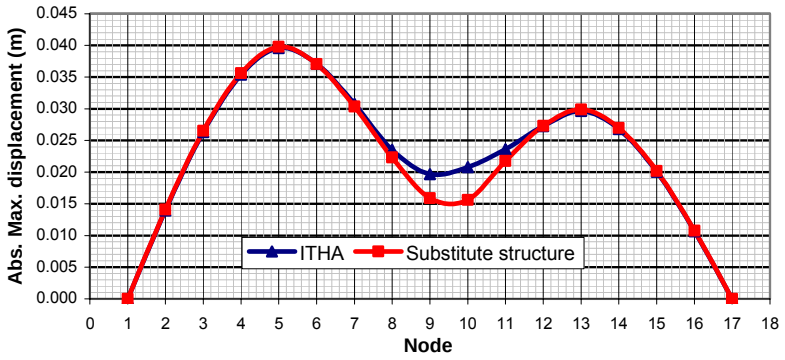

Figure 6.6. Distribution of absolute maximum displacements of bridge V213P, stage 2, signal 1

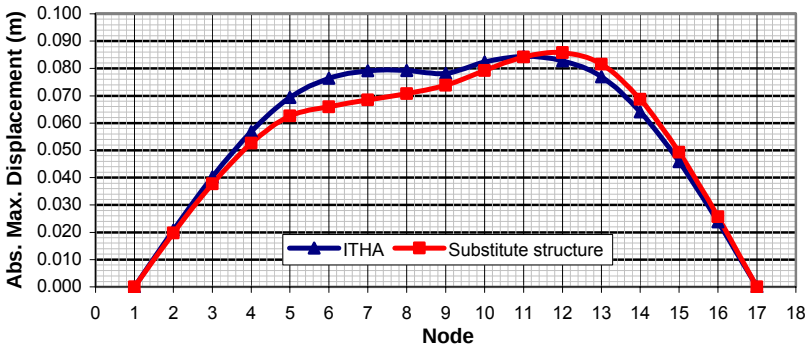

Figure 6.7. Distribution of absolute maximum displacements of bridge V213P, stage 3, signal 1

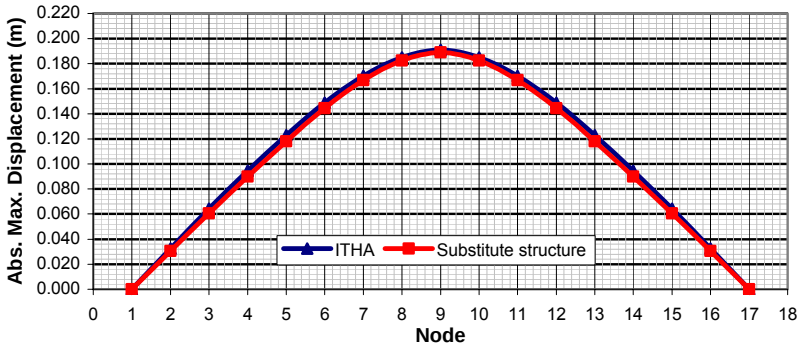

Figure 6.8. Distribution of absolute maximum displacements of bridge V232P, stage 3, signal 1

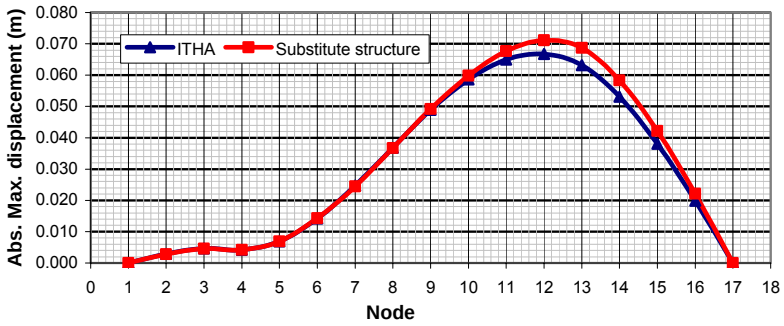

Figure 6.9. Distribution of absolute maximum displacements of bridge V123P, stage 2, signal 2

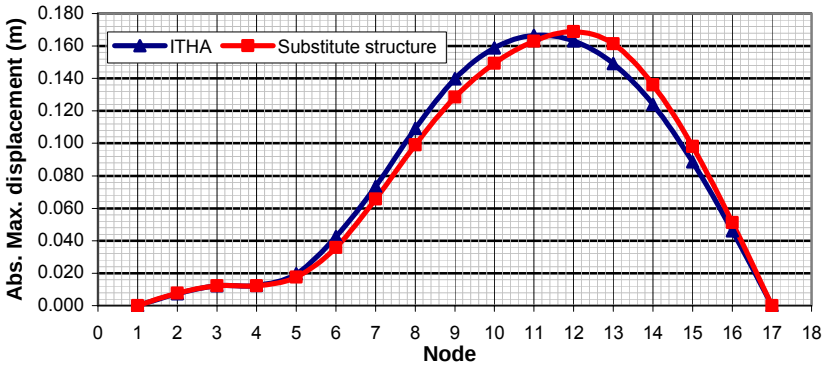

Figure 6.10. Distribution of absolute maximum displacements of bridge V123P, stage 3, signal 2

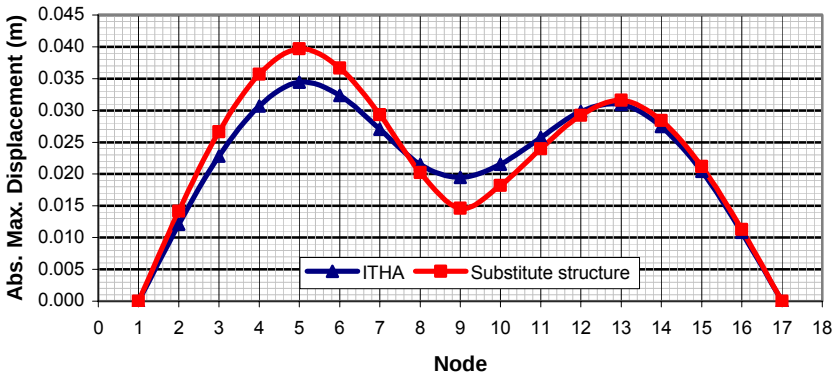

Figure 6.11. Distribution of absolute maximum displacements of bridge V213P, stage 2, signal 2

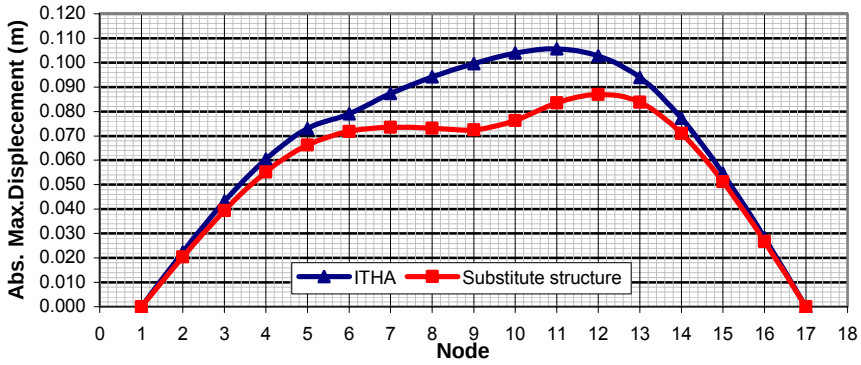

Figure 6.12. Distribution of absolute maximum displacements of bridge V213P, stage 3, signal 2

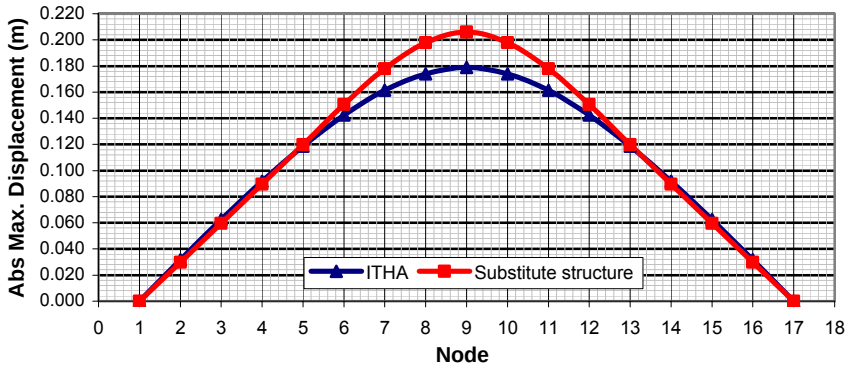

Figure 6.13. Distribution of absolute maximum displacements of bridge V232P, stage 3, signal 2

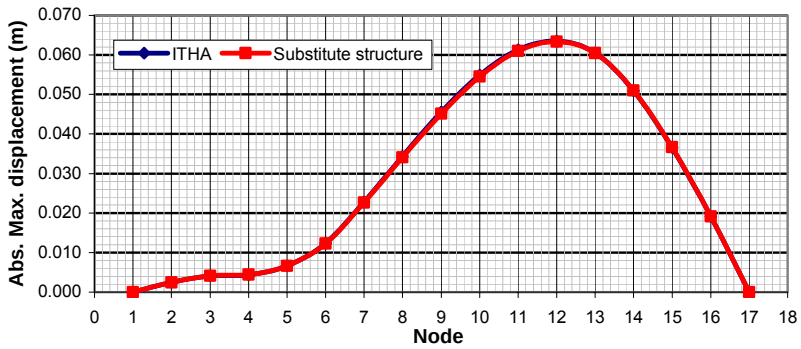

Figure 6.14. Distribution of absolute maximum displacements of bridge V123P, stage 2, signal 3

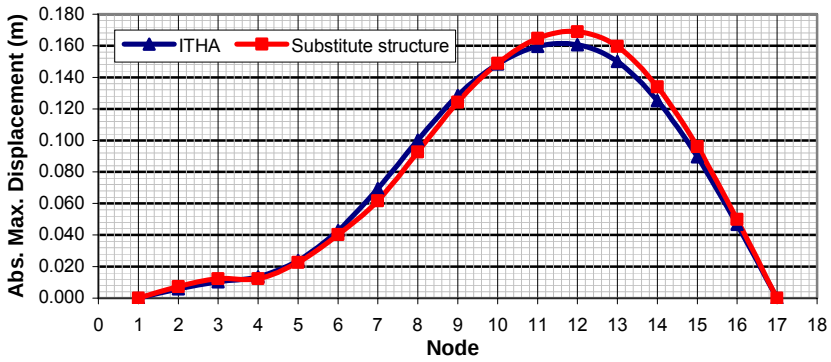

Figure 6.15. Distribution of absolute maximum displacements of bridge V123P, stage 3, signal 3

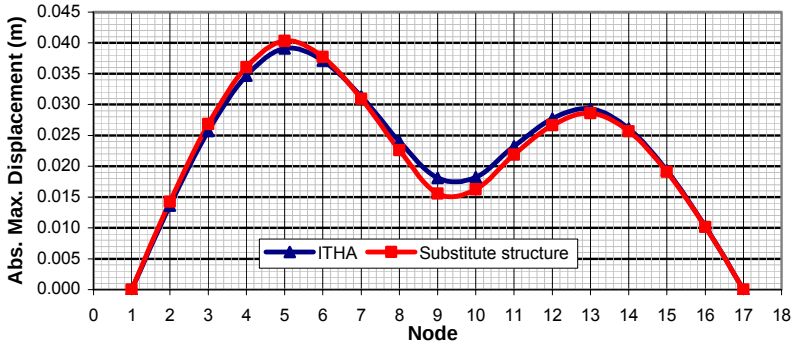

Figure 6.16. Distribution of absolute maximum displacements of bridge V213P, stage 2, signal 3

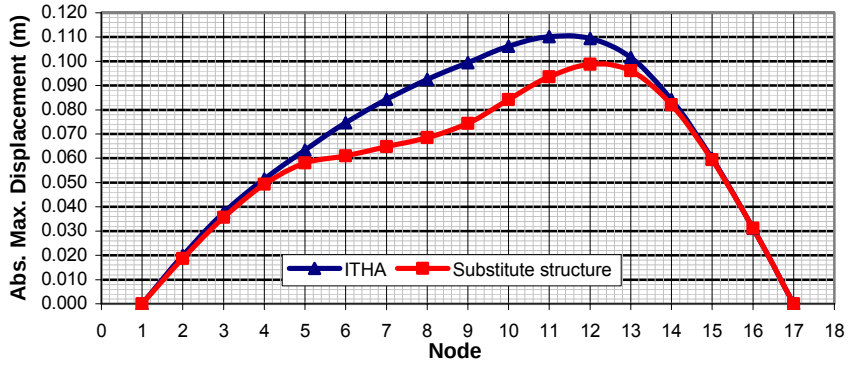

Figure 6.17. Distribution of absolute maximum displacements of bridge V213P, stage 3, signal 3

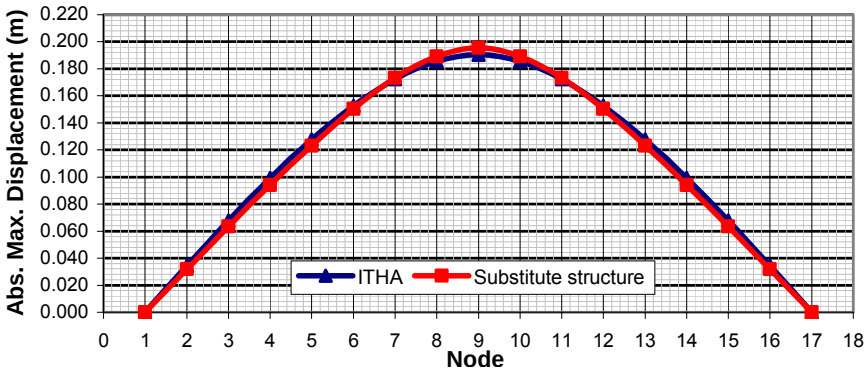

Figure 6.18. Distribution of absolute maximum displacements of bridge V232P, stage 3, signal 3

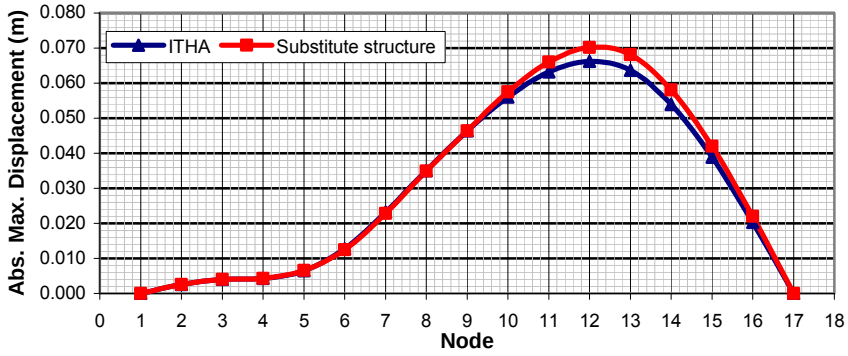

Figure 6.19. Distribution of absolute maximum displacements of bridge V123P, stage 2, signal 4

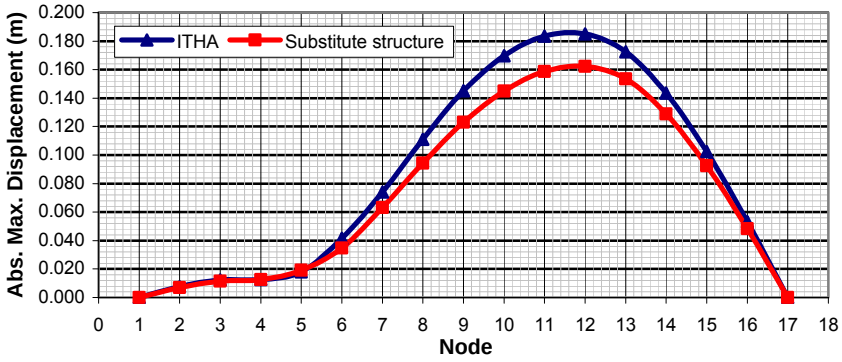

Figure 6.20. Distribution of absolute maximum displacements of bridge V123P, stage 3, signal 4

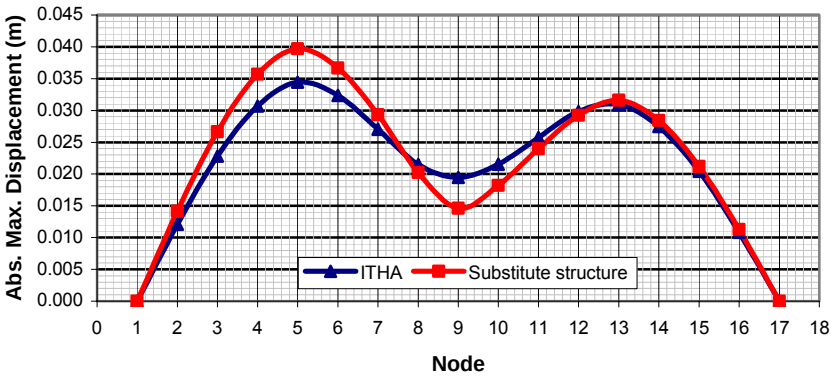

Figure 6.21. Distribution of absolute maximum displacements of bridge V213P, stage 2, signal 4

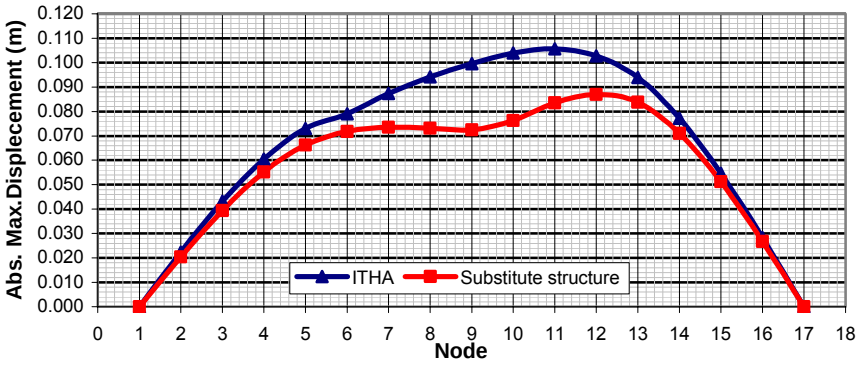

Figure 6.22. Distribution of absolute maximum displacements of bridge V213P, stage 3, signal 4

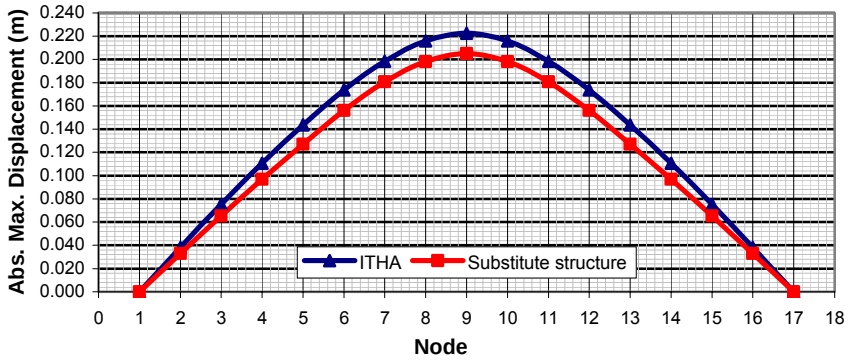

Figure 6.23. Distribution of absolute maximum displacements of bridge V232P, stage 3, signal 4

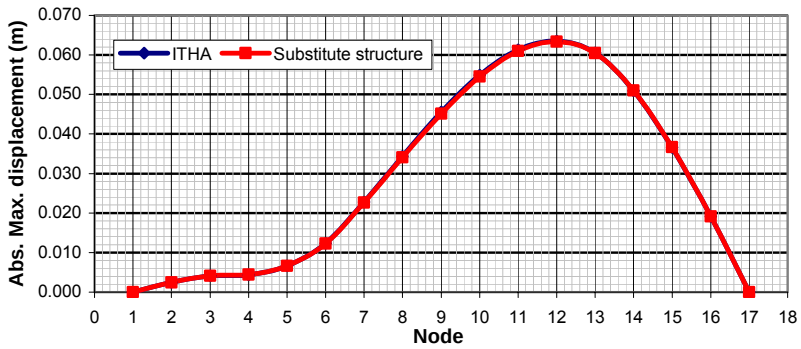

Figure 6.24. Distribution of absolute maximum displacements of bridge V123P, stage 2, signal 5

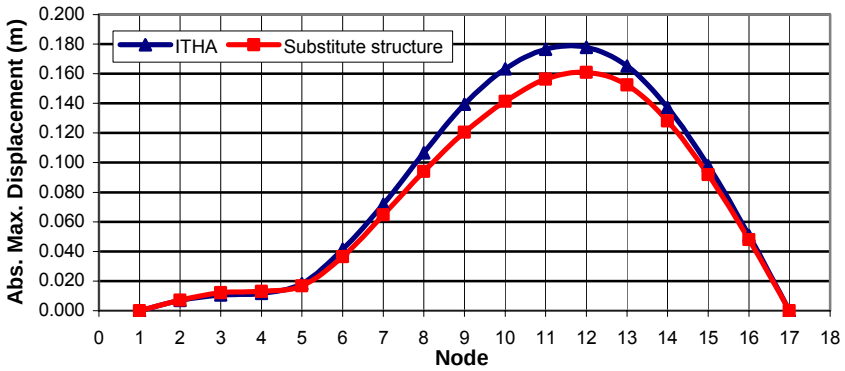

Figure 6.25. Distribution of absolute maximum displacements of bridge V123P, stage 3, signal 5

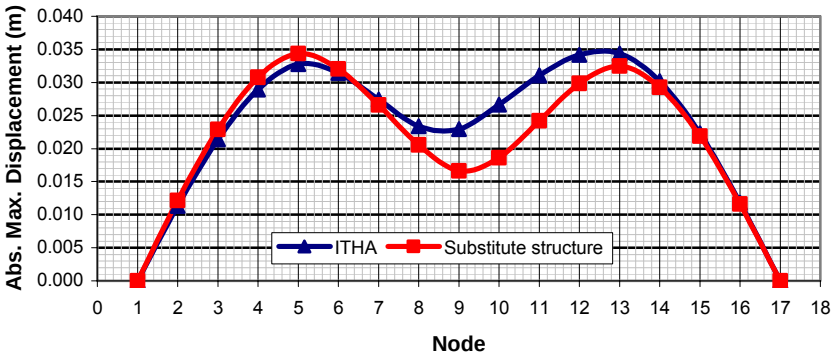

Figure 6.26. Distribution of absolute maximum displacements of bridge V213P, stage 2, signal 5

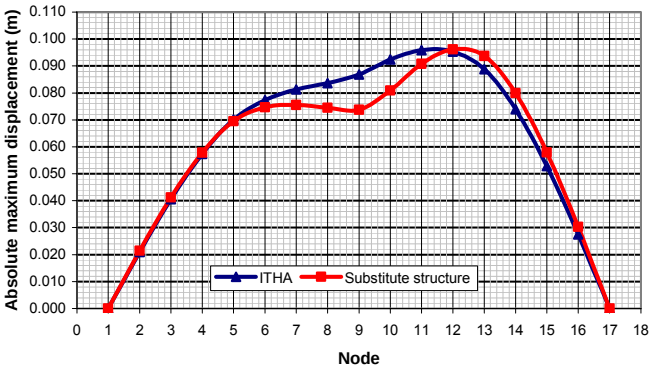

Figure 6.27. Distribution of absolute maximum displacements of bridge V213P, stage 3, signal 5

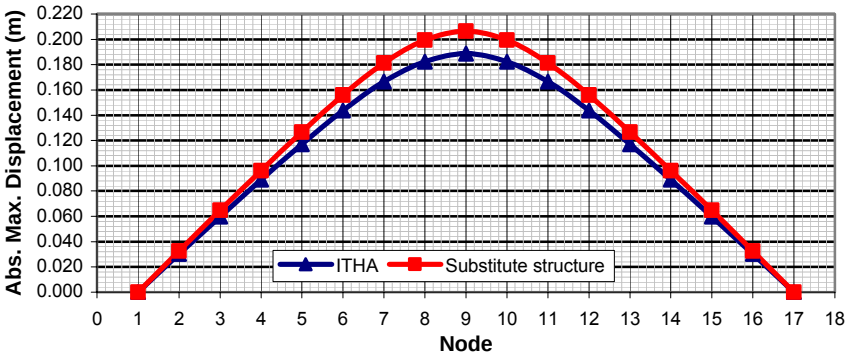

Figure 6.28. Distribution of absolute maximum displacements of bridge V232P, stage 3, signal 5

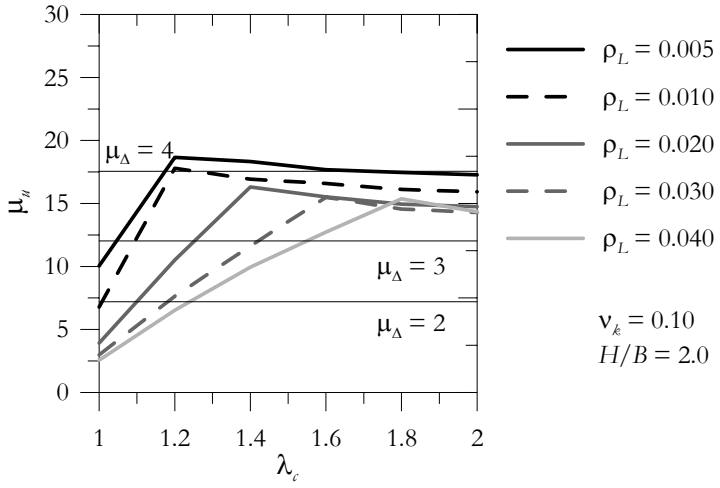

Figure 8.1. Proposed chart for the design of hollow rectangular piers with ν_k=0.10 and H/B=2.0, using displacement ductility, μ_Δ, as performance parameter, Paulotto et al. [2007b]

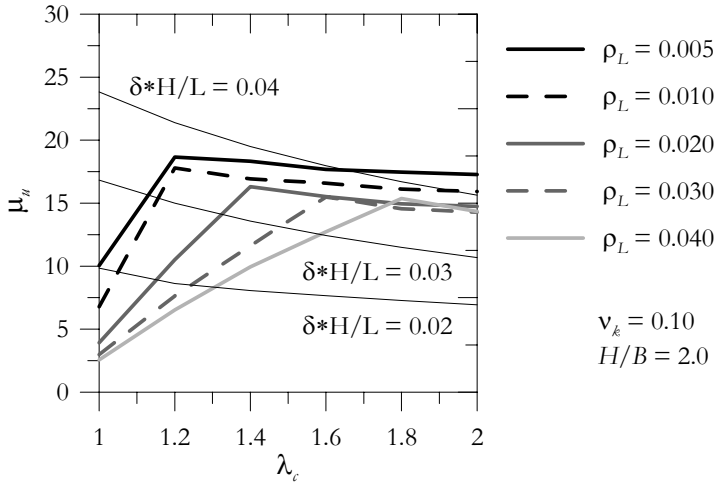

Figure 8.2. Proposed chart for the design of hollow rectangular piers with ν_k=0.10 and H/B=2.0 using drift, δ, as performance parameter., Paulotto et al. [2007b]

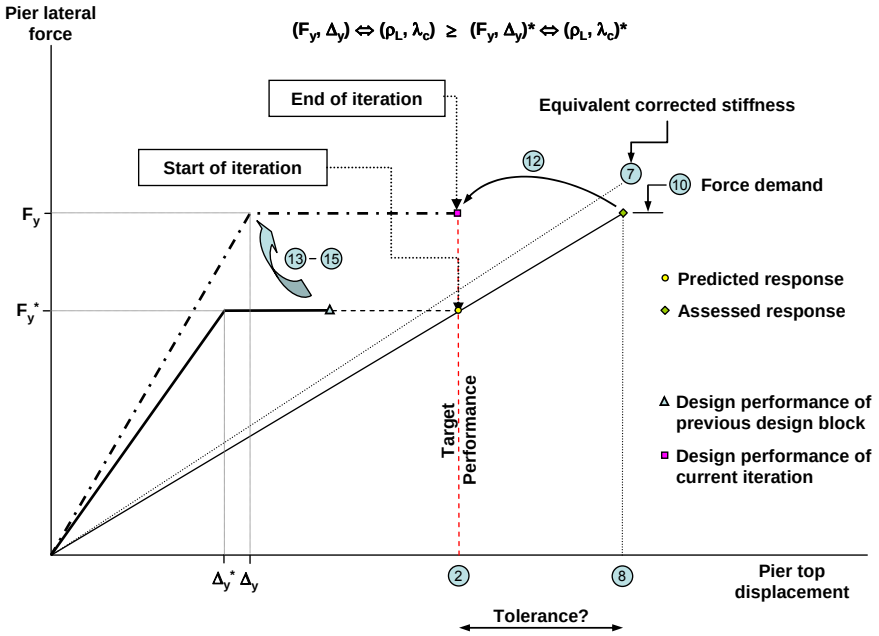

Figure 8.3. Displacement-Based Design: Step-by-step Iteration procedure

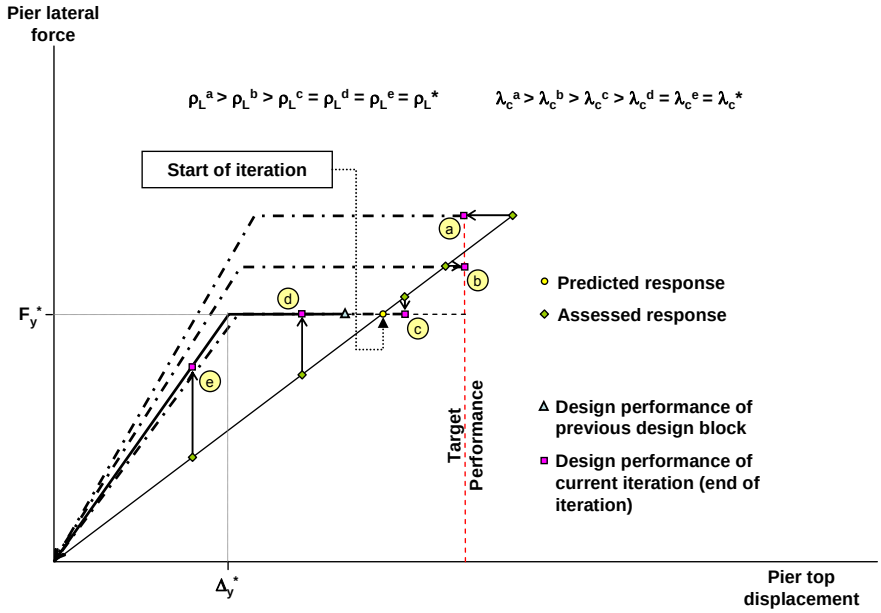

Figure 8.4. Displacement-Based Design: Examples of design performance solutions

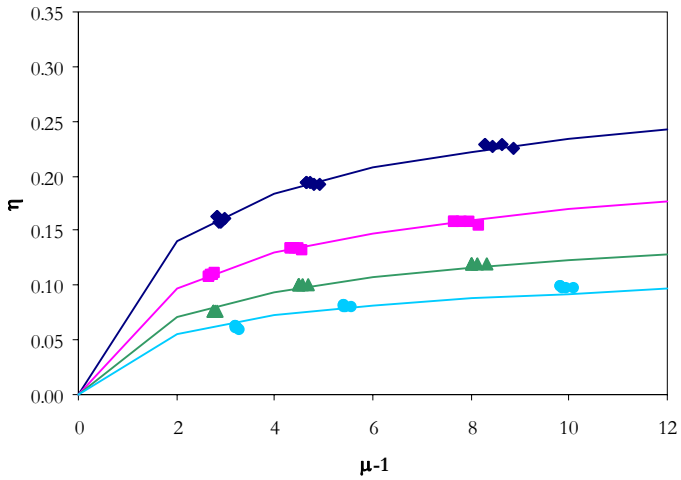

Figure 9.1. Hysteretic energy dissipated at the section level (ρ_L = 0.005) in terms of ductility for different axial load ratios (ν_k = 0.1, 0.2, 0.3 and 0.4; higher energy corresponding to lower values of ν_k): Comparison between analytical results (Fibre model, discrete points) and Takeda model (continuous line) for r = 0, β = 0.3 and α = 0.62, 0.79, 0.88 and 0.93

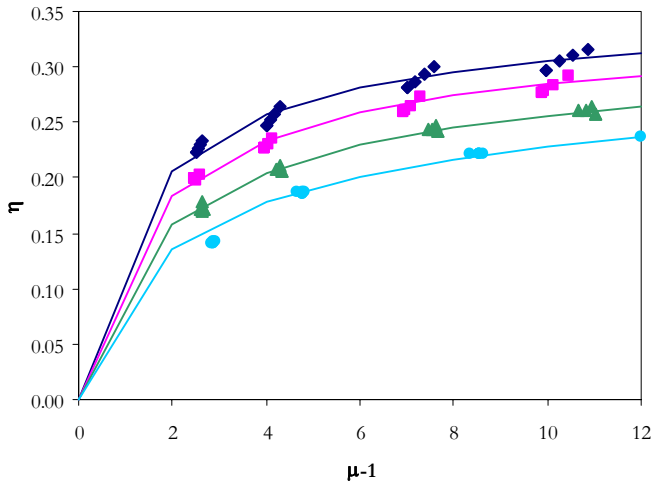

Figure 9.2. Hysteretic energy dissipated at the section level (ρ_L = 0.010) in terms of ductility for different axial load ratios (ν_k = 0.1, 0.2, 0.3 and 0.4; higher energy corresponding to lower values of ν_k): Comparison between analytical results (Fibre model, discrete points) and Takeda model (continuous line) for r = 0, β = 0.3 and α = 0.47, 0.61, 0.75 and 0.82

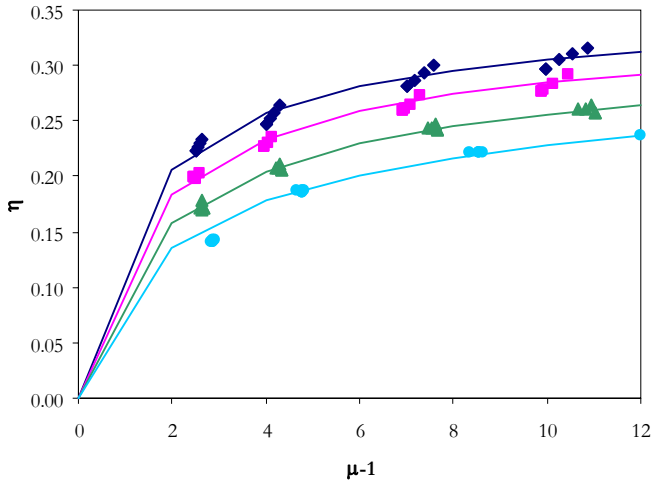

Figure 9.3. Hysteretic energy dissipated at the section level (ρ_L = 0.020) in terms of ductility for different axial load ratios (ν_k = 0.1, 0.2, 0.3 and 0.4; higher energy corresponding to lower values of ν_k): Comparison between analytical results (Fibre model, discrete points) and Takeda model (continuous line) for r = 0, β = 0.3 and α = 0.28, 0.41, 0.54 and 0.64

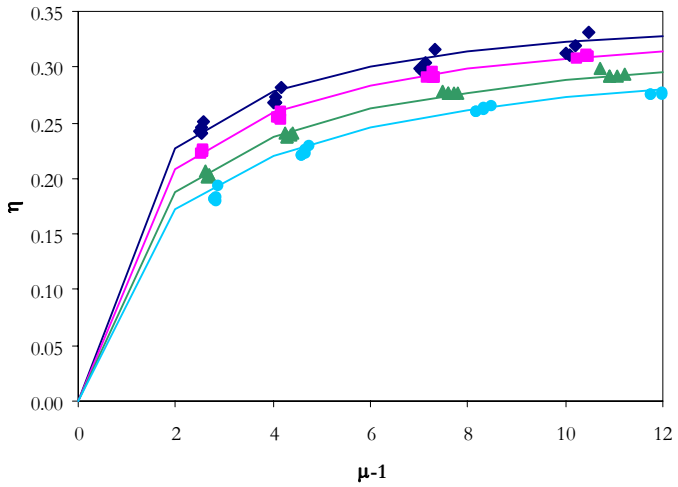

Figure 9.4. Hysteretic energy dissipated at the section level (ρ_L = 0.030) in terms of ductility for different axial load ratios (ν_k = 0.1, 0.2, 0.3 and 0.4; higher energy corresponding to lower values of ν_k): Comparison between analytical results (Fibre model, discrete points) and Takeda model (continuous line) for r = 0, β = 0.3 and α = 0.13, 0.26, 0.39 and 0.47

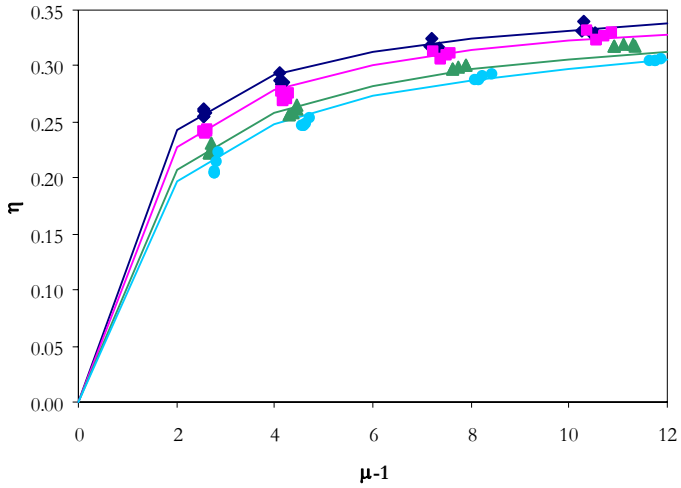

Figure 9.5. Hysteretic energy dissipated at the section level (ρ_L = 0.040) in terms of ductility for different axial load ratios (ν_k = 0.1, 0.2, 0.3 and 0.4; higher energy corresponding to lower values of ν_k): Comparison between analytical results (Fibre model, discrete points) and Takeda model (continuous line) for r = 0, β = 0.3 and α = 0.01, 0.13, 0.27 and 0.33

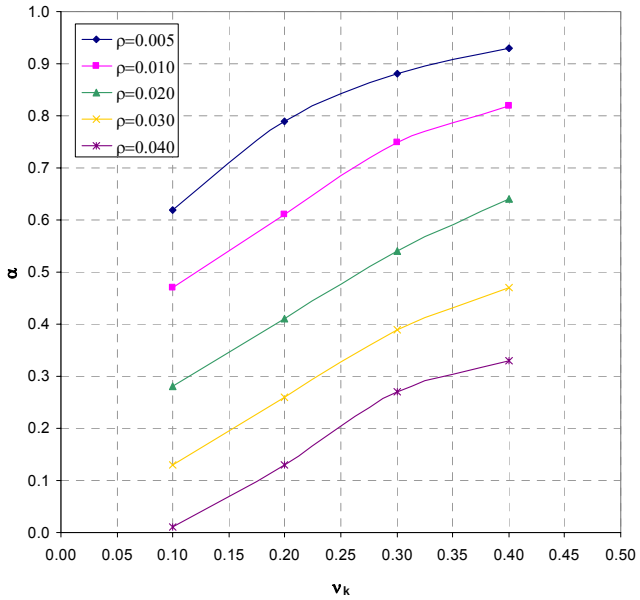

Figure 9.6. Takeda Model (r = 0, β = 0.3): Values of α as a function of axial load ratio ν_k for different levels of longitudinal reinforcement ρ_L to match the energy dissipated by the Fibre Model.

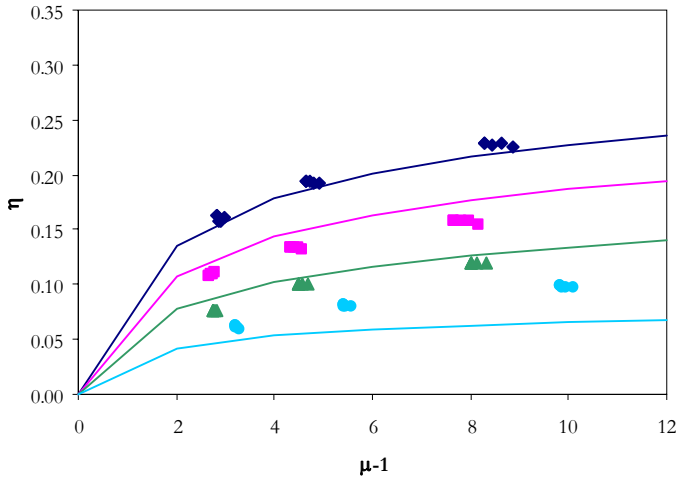

Figure 9.7. Hysteretic energy dissipated at the section level (ρ_L = 0.005) in terms of ductility for different axial load ratios (ν_k = 0.1, 0.2, 0.3 and 0.4; higher energy corresponding to lower values of ν_k): Comparison between analytical results (Fibre model, discrete points) and Takeda model (continuous line) for r = 0, β = 0.3 and α from Eq. (9.2)

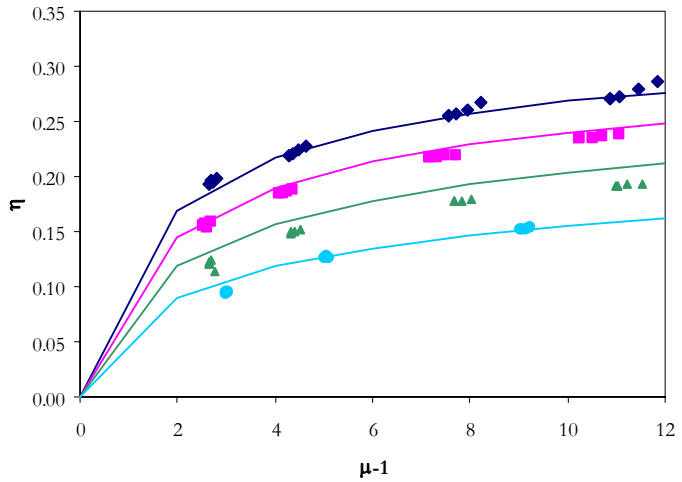

Figure 9.8. Hysteretic energy dissipated at the section level (ρ_L = 0.010) in terms of ductility for different axial load ratios (ν_k = 0.1, 0.2, 0.3 and 0.4; higher energy corresponding to lower values of ν_k): Comparison between analytical results (Fibre model, discrete points) and Takeda model (continuous line) for r = 0, β = 0.3 and α from Eq. (9.2)

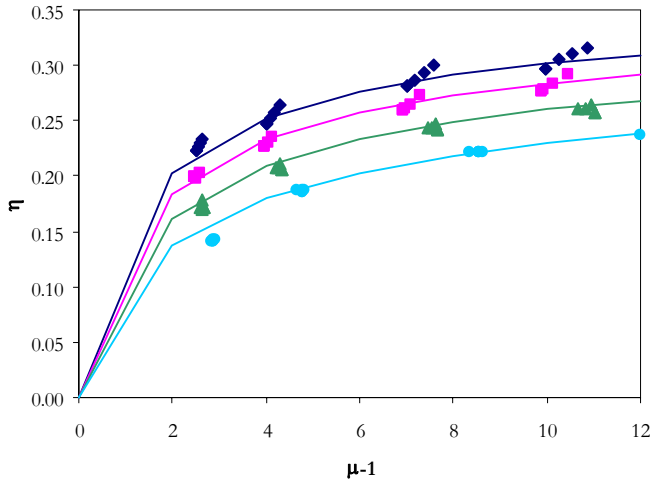

Figure 9.9 Hysteretic energy dissipated at the section level (ρ_L = 0.020) in terms of ductility for different axial load ratios (ν_k = 0.1, 0.2, 0.3 and 0.4; higher energy corresponding to lower values of ν_k): Comparison between analytical results (Fibre model, discrete points) and Takeda model (continuous line) for r = 0, β = 0.3 and α from Eq. (9.2)

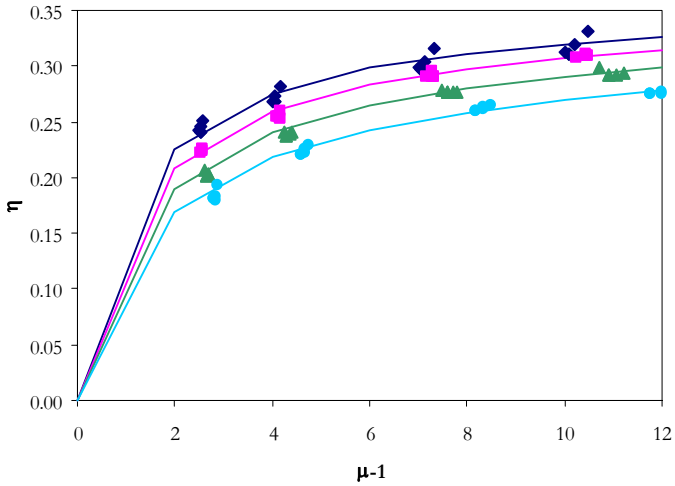

Figure 9.10. Hysteretic energy dissipated at the section level (ρ_L = 0.030) in terms of ductility for different axial load ratios (ν_k = 0.1, 0.2, 0.3 and 0.4; higher energy corresponding to lower values of ν_k): Comparison between analytical results (Fibre model, discrete points) and Takeda model (continuous line) for r = 0, β = 0.3 and α from Eq. (9.2)

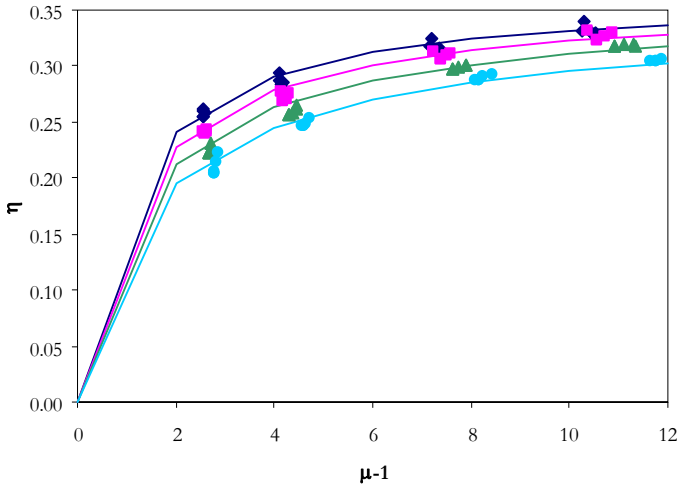

Figure 9.11. Hysteretic energy dissipated at the section level (ρ_L = 0.040) in terms of ductility for different axial load ratios (ν_k = 0.1, 0.2, 0.3 and 0.4; higher energy corresponding to lower values of ν_k): Comparison between analytical results (Fibre model, discrete points) and Takeda model (continuous line) for r = 0, β = 0.3 and α from Eq. (9.2)

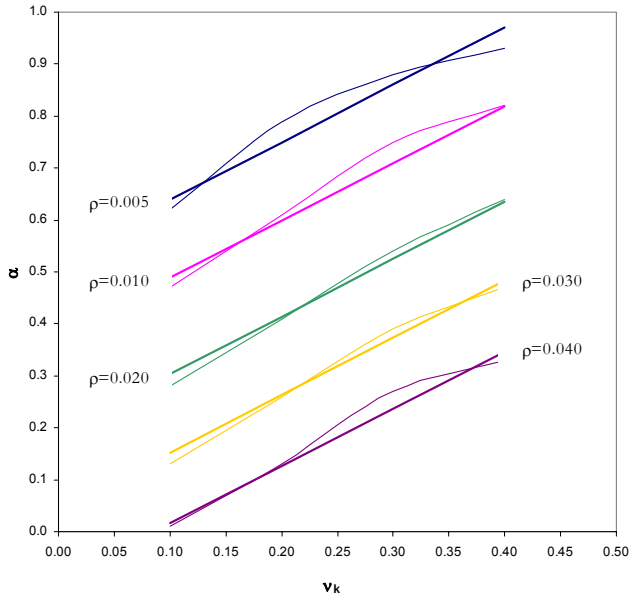

Figure 9.12 Takeda Model (r = 0, β = 0.3): Values of α as a function of axial load ratio ν_k for different levels of longitudinal reinforcement ρ_L; comparison between best fit with Fibre model and Eq. (9.2)

European Commission

EUR 23066 EN – Joint Research Centre – Institute for the Protection and Security of the Citizen
Title: Validation of simplified procedures for predicting global response in the context of DBD of bridges, including the flexibility of foundations / Case study comparison of DBD iterative procedures for bridges
Author(s): Fabio TAUCER, Gustavo AYALA, Carlo PAULOTTO
Luxembourg: Office for Official Publications of the European Communities
2007 – 59 pp. – 21 x 29.7 cm
EUR – Scientific and Technical Research series – ISSN 1018-5593

Abstract
The present report collects the work performed in Deliverable 112 “Validation of simplified procedures for predicting global response in the context of DBD of bridges, including the flexibility of foundations” and in the chapter corresponding to Displacement Based Design of Deliverable 113 “Case study comparison of DBD iterative procedures for bridges” of the LESSLOSS Project, dealing with three main subjects: verifying that the concept of the Substitute Structure constitutes a valid means of predicting the response of a bridge structure undergoing plastic deformations; formulating a procedure for the displacement based design performance of bridges; defining the parameters of a Takeda Model to be used within the context of non-linear time history analysis of bridges with RC rectangular hollow columns.

The mission of the JRC is to provide customer-driven scientific and technical support for the conception, development, implementation and monitoring of EU policies. As a service of the European Commission, the JRC functions as a reference centre of science and technology for the Union. Close to the policy-making process, it serves the common interest of the Member States, while being independent of special interests, whether private or national.

JRC
EUROPEAN COMMISSION

Publications Office
Publications.eu.int